Characterization of GPS L-band scintillations under different types of ESF irregularities using co-located ionosonde observations

S. Sripathi, S. Sreeba, Ram Singh and S. Banola

Indian Institute of Geomagnetism, Navi Mumbai, India.
Email: ssripathi.iig@gmail.com

Beacon satellite Symposium during 26 June to 01 July 2016 at ICTP, Trieste, Italy

Outline of the presentation

1. Objectives
2. Introduction
3. Data sets used in the analysis
4. Variability of GPS scintillations during low to moderate solar activity periods
5. Variability of Ionosonde observations of ESF and their relation to GPS scintillations at Tirunelveli
6. Correlation of EEJ strength and Virtual height during (non) scintillations periods
7. Summary and conclusions

OBJECTIVE **of this study is to investigate the day-to-day variability of GPS scintillations that are caused due to refractive index fluctuations in the ionosphere under different solar flux levels. Also understand the role of (a) Pre-Reversal Enhancement (PRE) of the zonal electric field and (b) EEJ strength in the generation of scintillations/irregularities.**

Introduction

- **The ionospheric variability under quiet and disturbed conditions have been studied extensively due to its impact on the radio wave propagation.**

- **However, still the day-to-day variability of the ionospheric processes and their impact on the EM wave propagation is puzzling.**

- **Since ionospheric processes (low latitude) such as EEJ, EIA and ESF are elctrodynamically coupled together, we need to understand their coupling to understand the ionospheric effects on the radio propagation.**

Introduction continued...

Diffuse ionogram echoes during spread F event

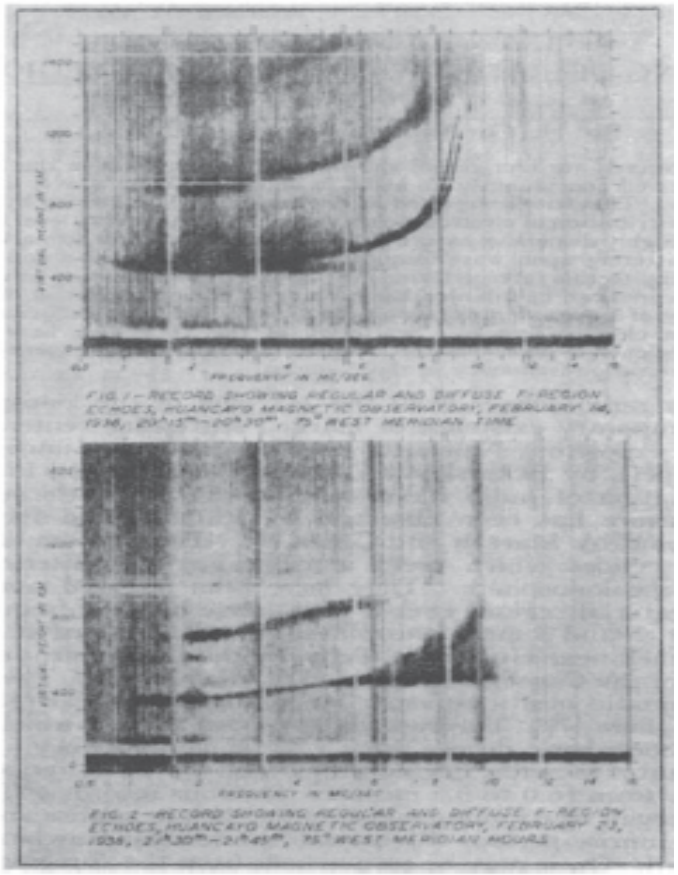

Booker and Wells, 1934

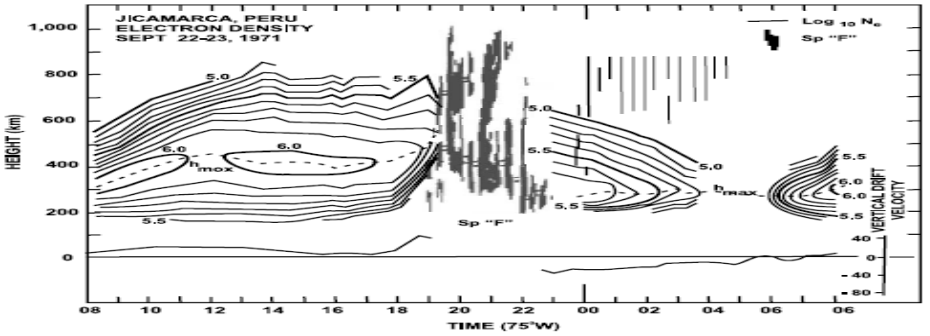

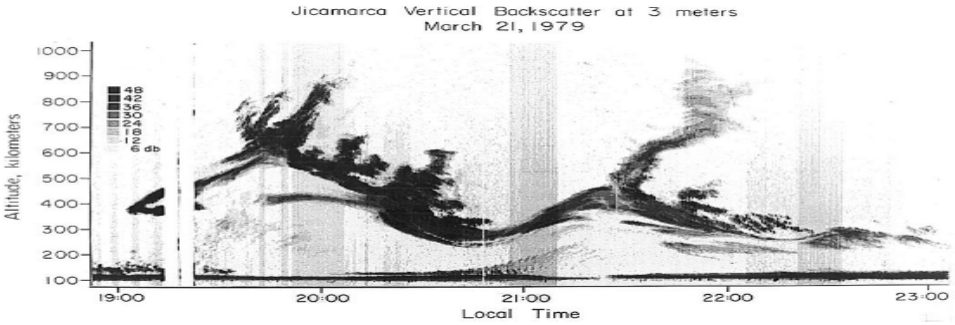

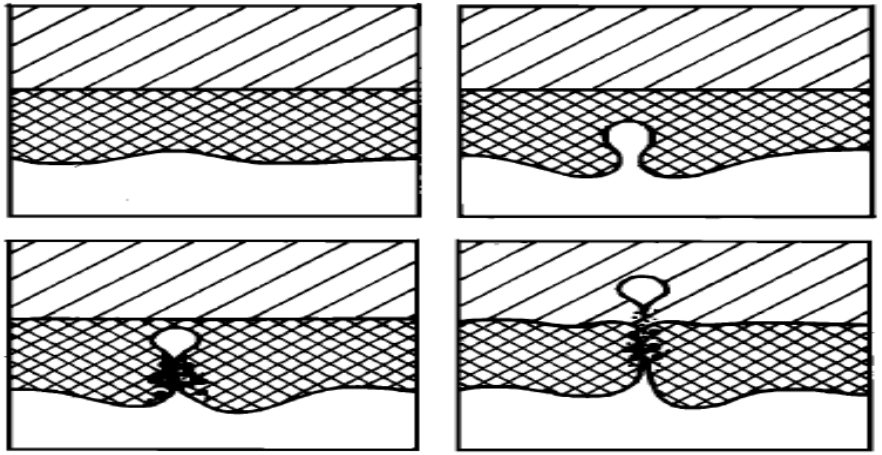

Woodman and La Hoz, JGR, 1976

Introduction continued...

Gravitational Rayleigh-Taylor Instability - Equatorial Spread-F

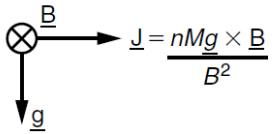

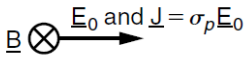

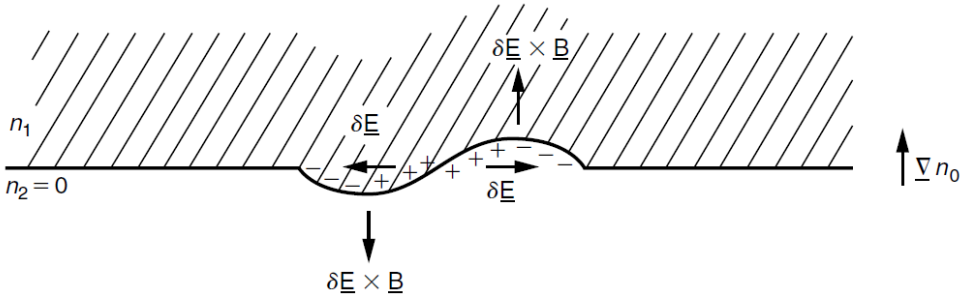

Gravity (g) ➔ $\vec{v}_g = \frac{m}{q}\frac{\vec{g} \times \vec{B}}{B^2}$

Linear Growth rate of instability, $\gamma_g = \frac{1}{L}\frac{g}{\nu_{in}}$

$$\frac{1}{L} = \frac{1}{N} \cdot \frac{dN}{dZ}$$

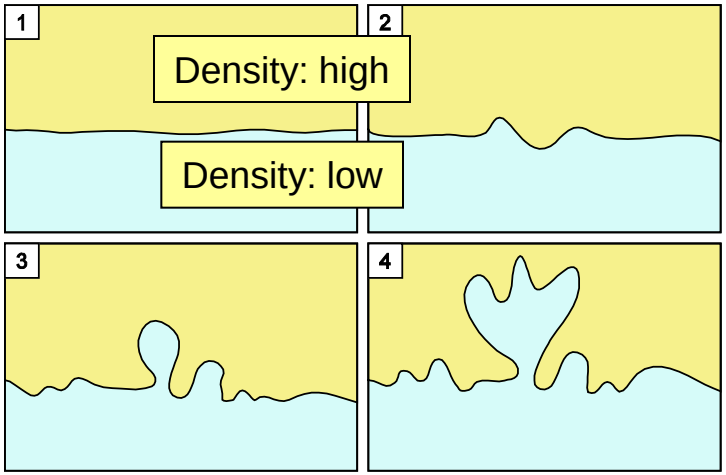

Development of plasma bubbles

L = inverse gradient scale length

Introduction continued...

The main parameters that affect the growth of the R-T Instability

Growth rate of the RT instability

$$\gamma = \frac{\Sigma_{P,0}^{F}}{\Sigma_{P,0}^{E} + \Sigma_{P,0}^{F}} \left(\vec{\mathbf{v}}_p - \vec{\mathbf{u}}_n - \frac{\vec{\mathbf{g}}}{\nu_{in}} \right) \bullet \frac{1}{N} \frac{\partial N}{\partial h} - R$$

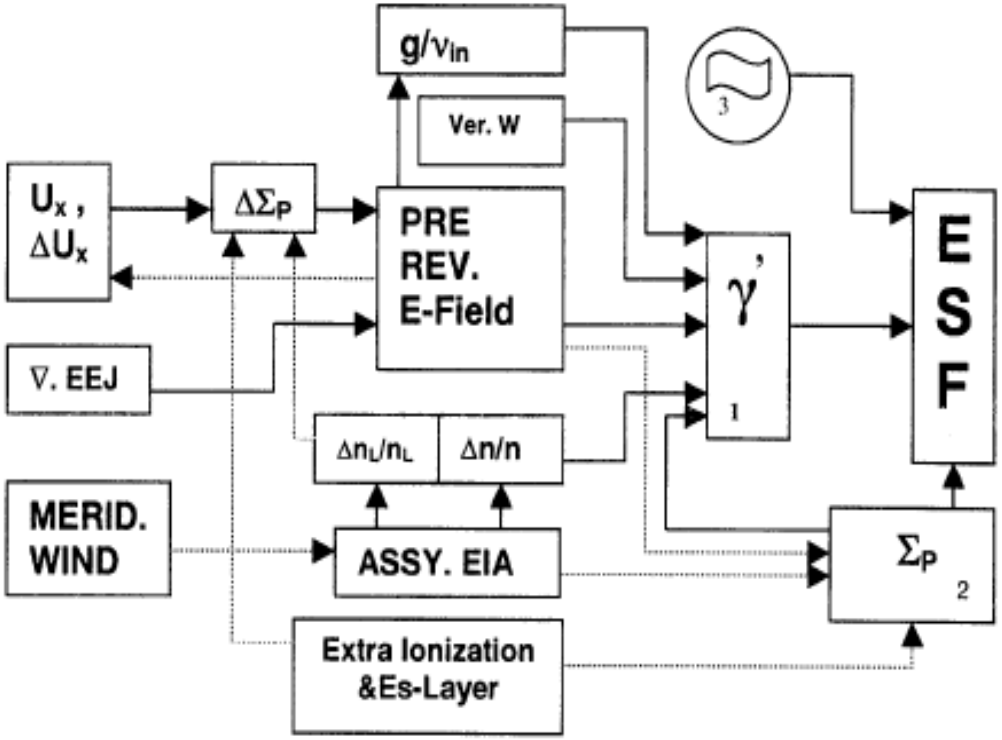

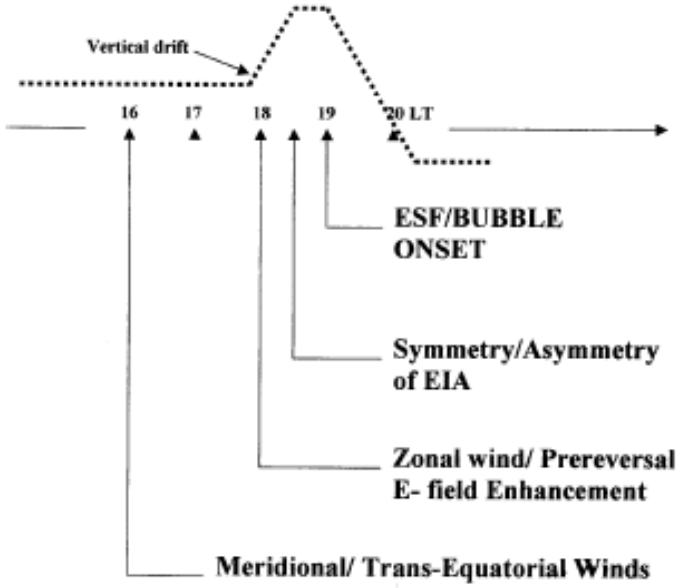

Abdu, JASTP, 2001

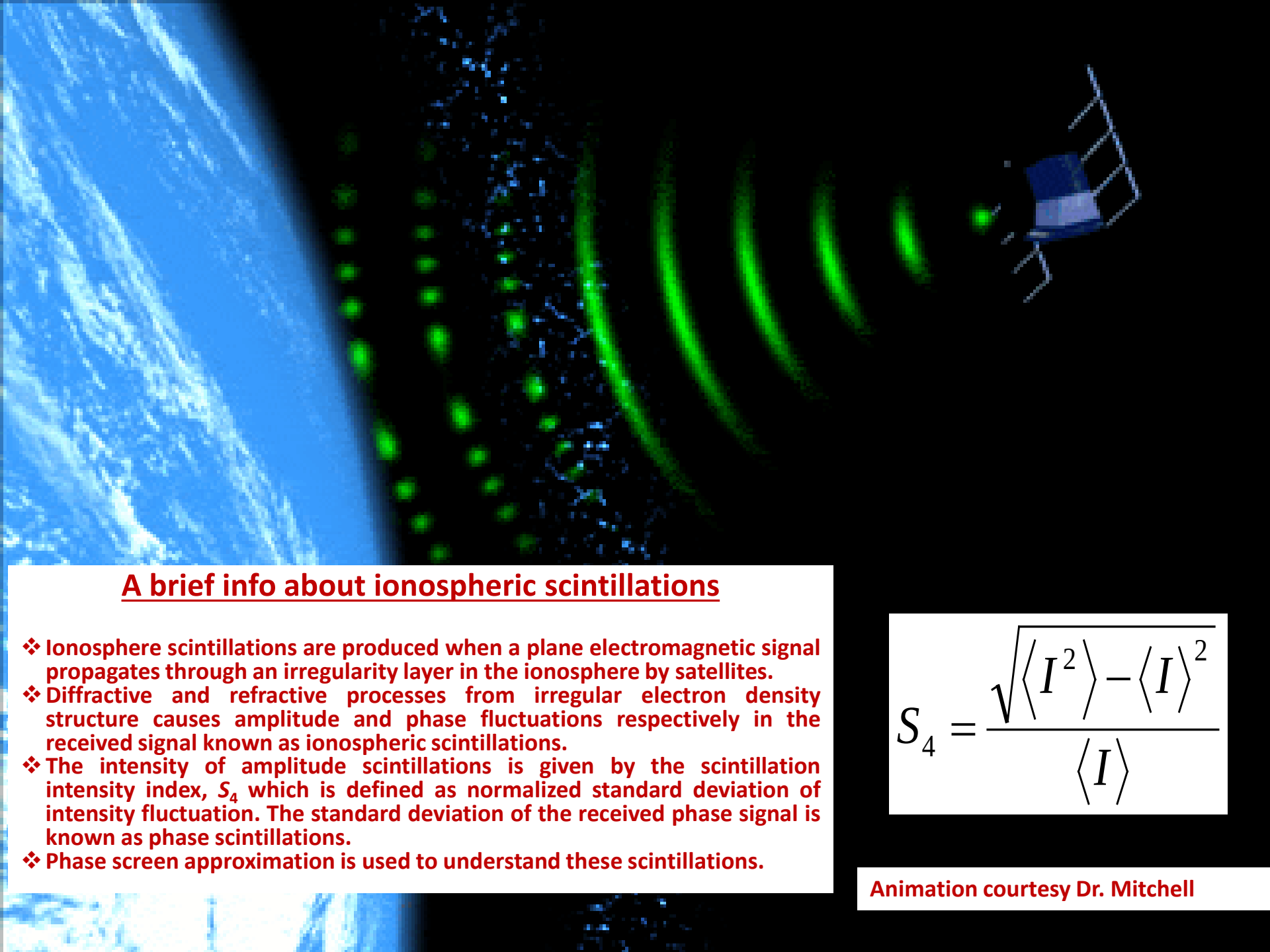

A brief info about ionospheric scintillations

- Ionosphere scintillations are produced when a plane electromagnetic signal propagates through an irregularity layer in the ionosphere by satellites.
- Diffractive and refractive processes from irregular electron density structure causes amplitude and phase fluctuations respectively in the received signal known as ionospheric scintillations.
- The intensity of amplitude scintillations is given by the scintillation intensity index, S_4 which is defined as normalized standard deviation of intensity fluctuation. The standard deviation of the received phase signal is known as phase scintillations.
- Phase screen approximation is used to understand these scintillations.

$$S_4 = \frac{\sqrt{\langle I^2 \rangle - \langle I \rangle^2}}{\langle I \rangle}$$

Animation courtesy Dr. Mitchell

Locations in India

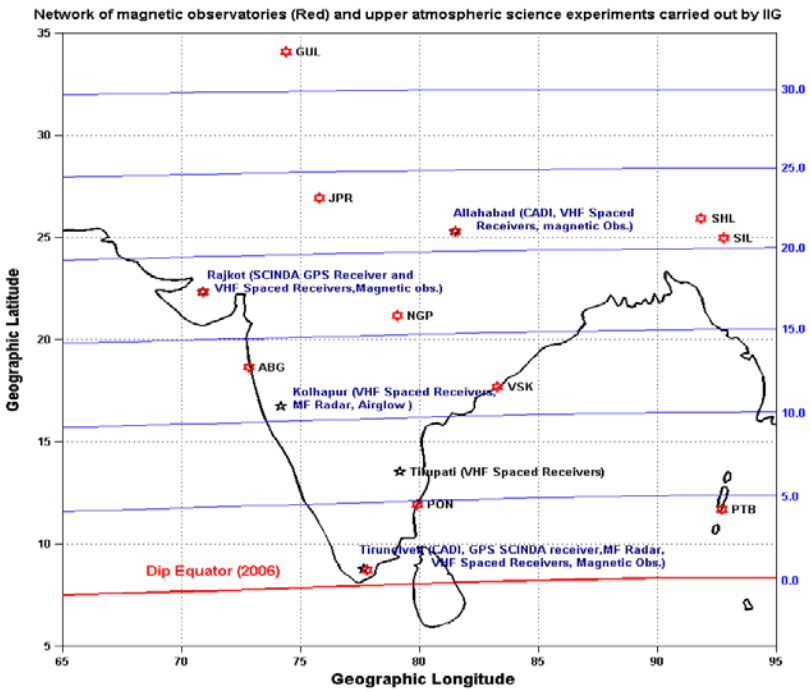

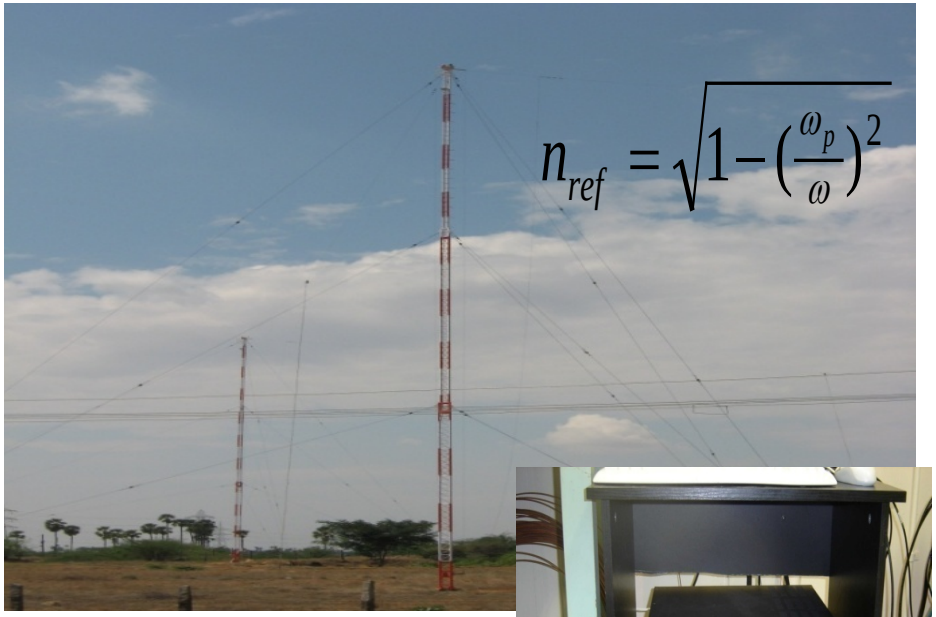

$$n_{ref} = \sqrt{1-\left(\frac{\omega_p}{\omega}\right)^2}$$

Ionosonde

GPS SCINDA network

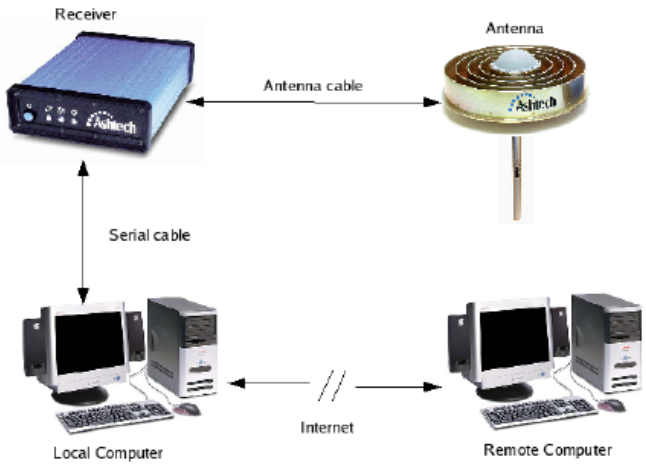

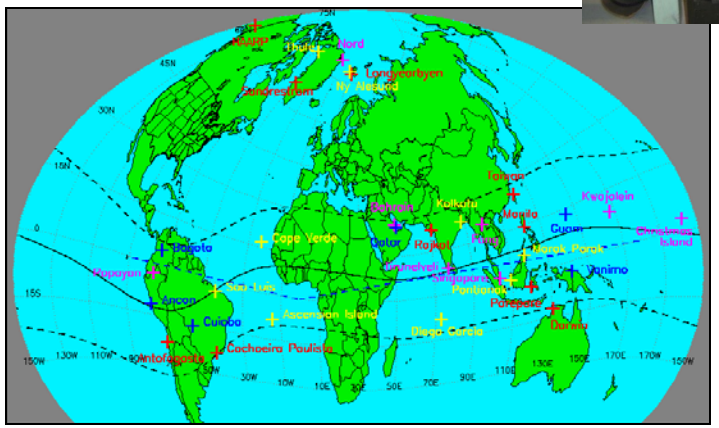

Description of the data sets

- SCINDA GPS receiver data at Tirunelveli, Indian region during the years 2007-2013.
- Canadian Digital Ionosonde (CADI) data from Tirunelveli, an equatorial station
- Delta H values over Indian region
- Geomagnetic indices like kp, Ap and solar indices like solar flux and sunspot numbers

GPS L-band scintillations during 2007-2013 over Tirunelveli

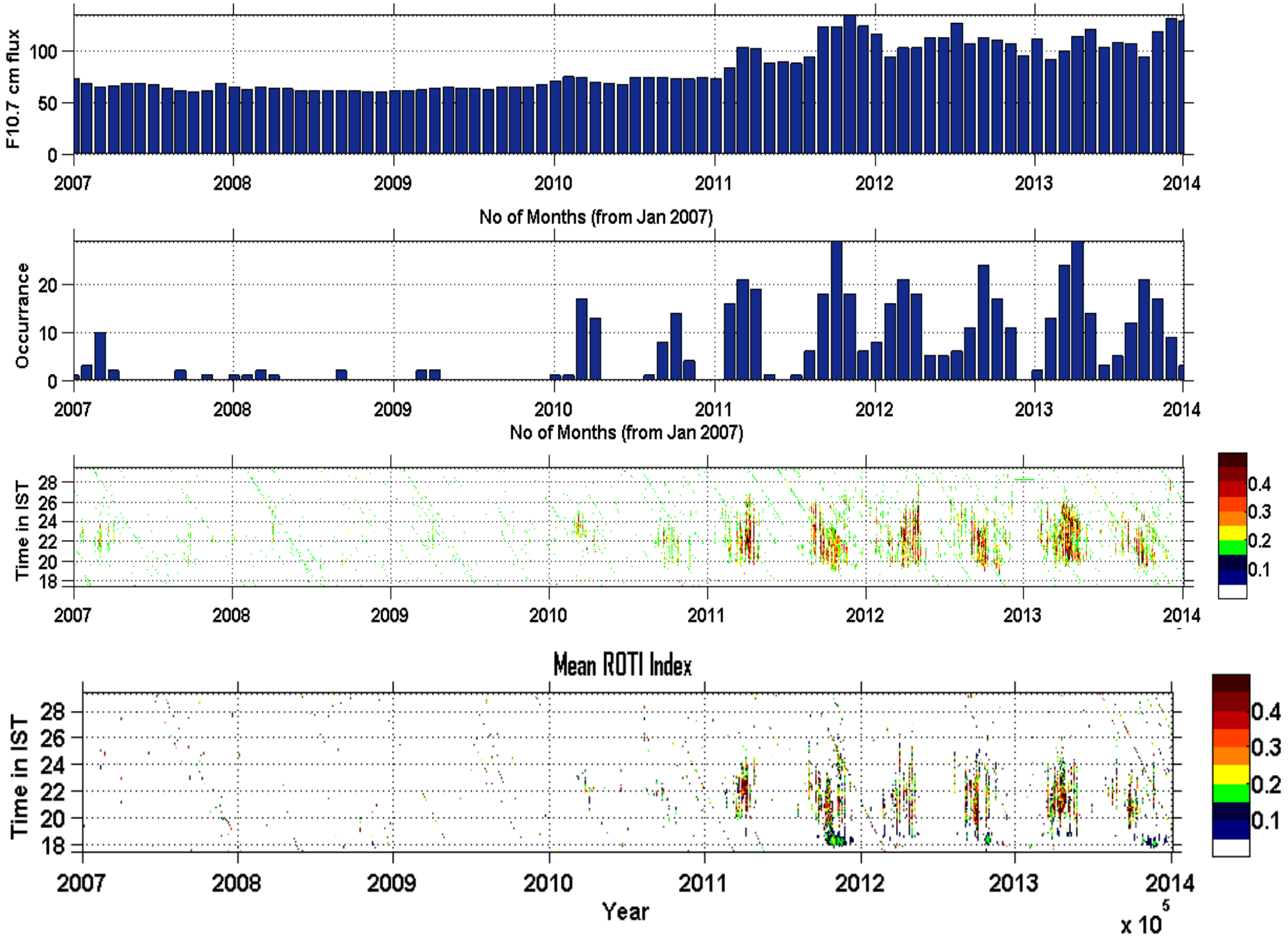

Typical examples of Range and Frequency spread F irregularities in ionograms

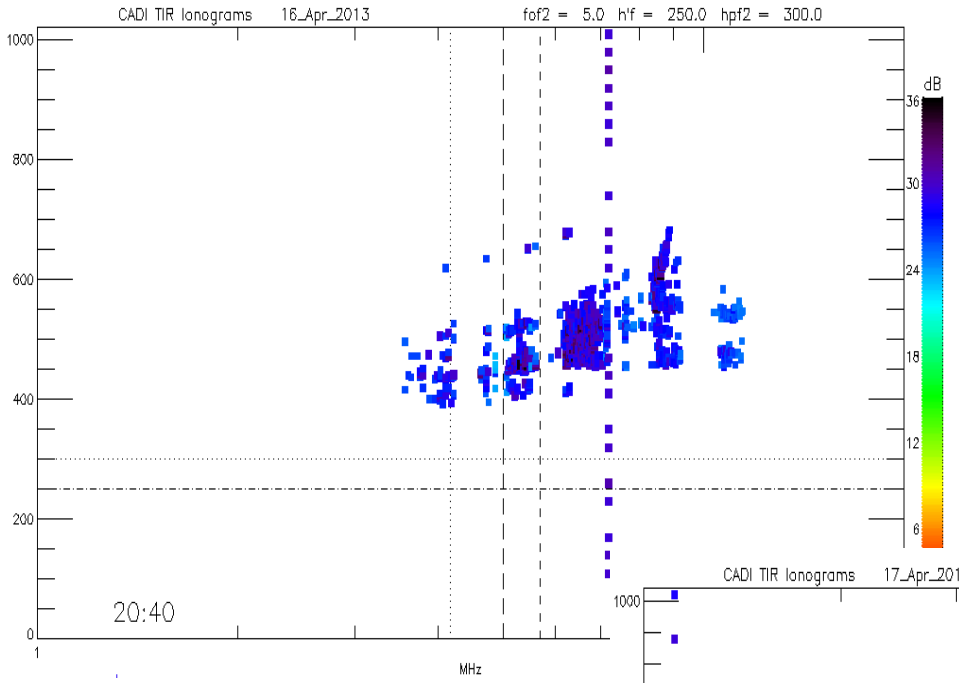

Range spread F

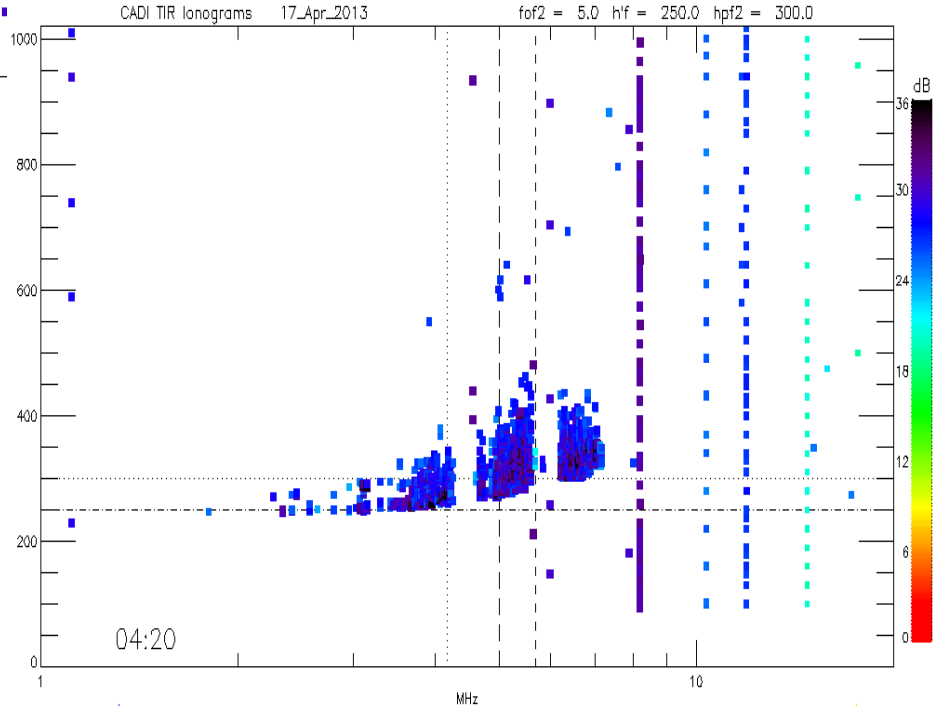

Frequency spread F

Satellite traces in the ionograms prior to spread F. This is caused due to corrugation in the F layer by LSWS

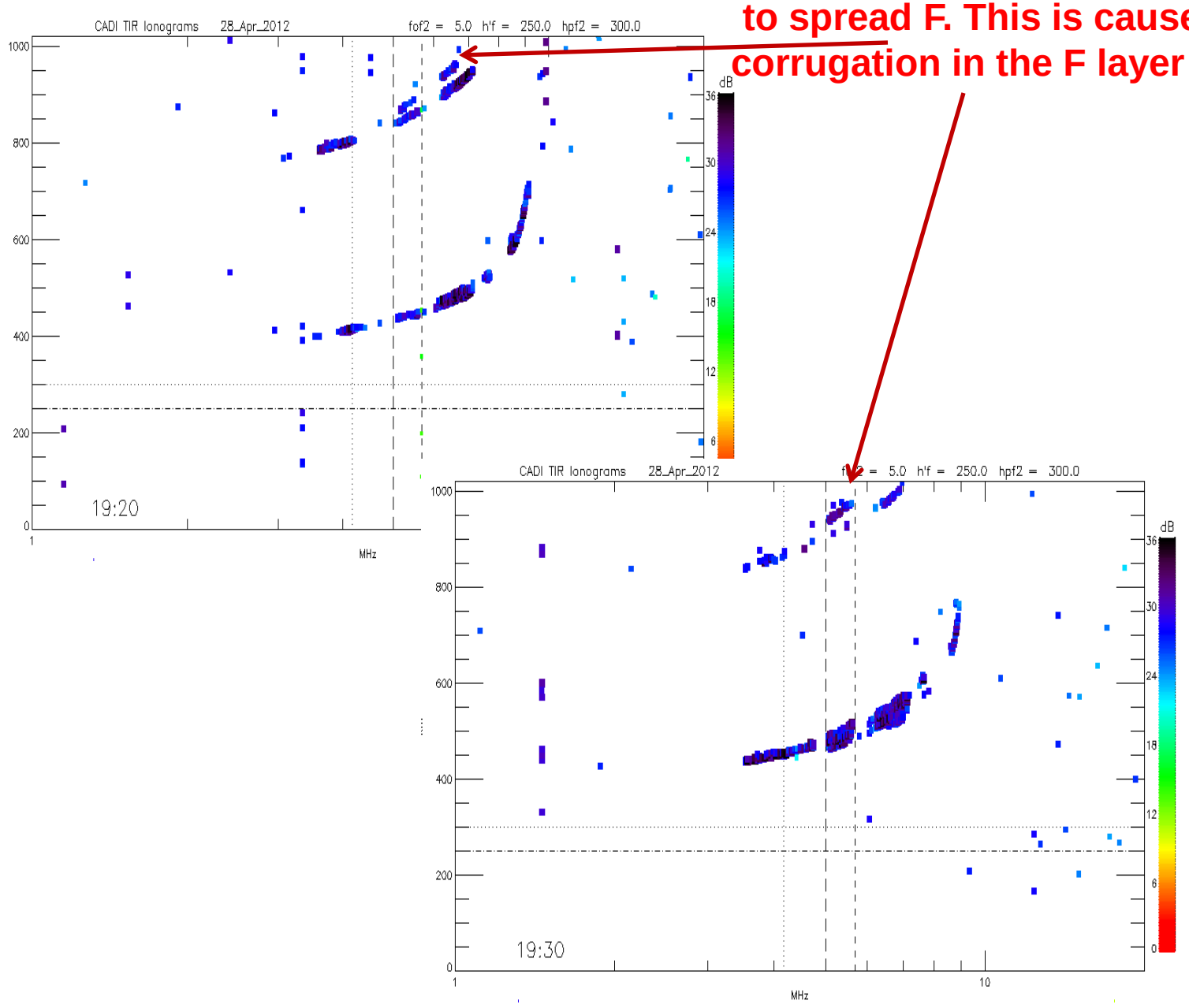

Typical example of ionospheric scintillations at L-band and the TEC fluctuations during an ESF event

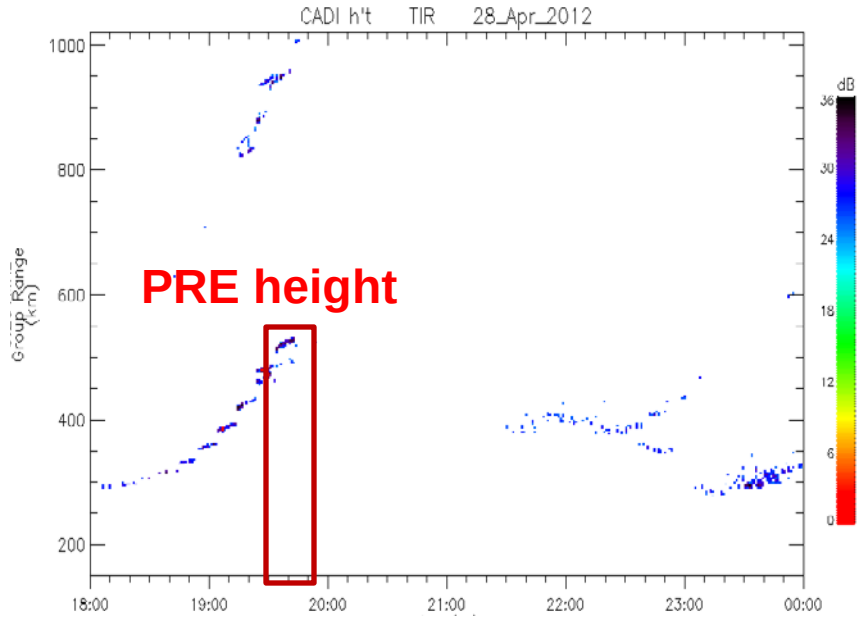

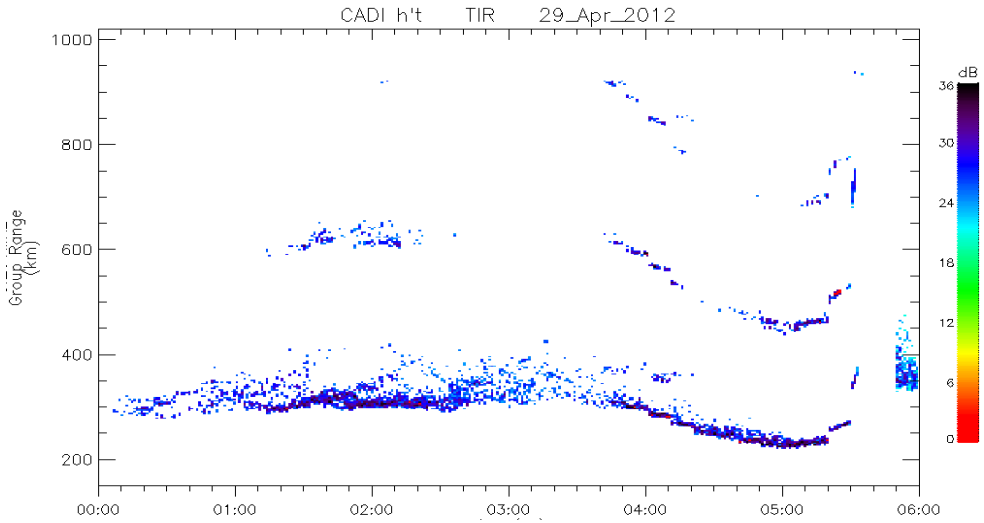

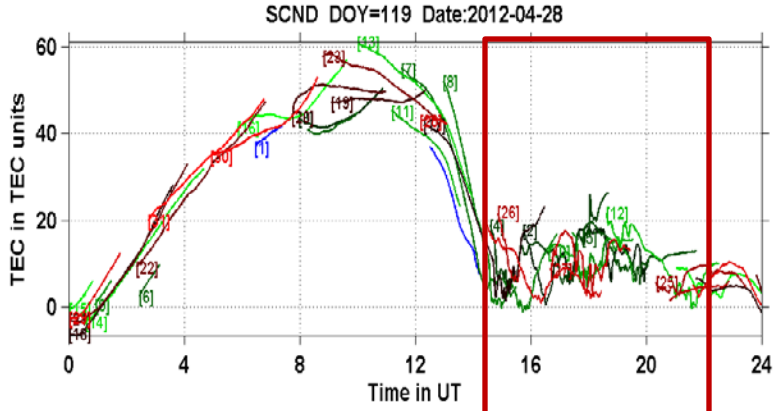

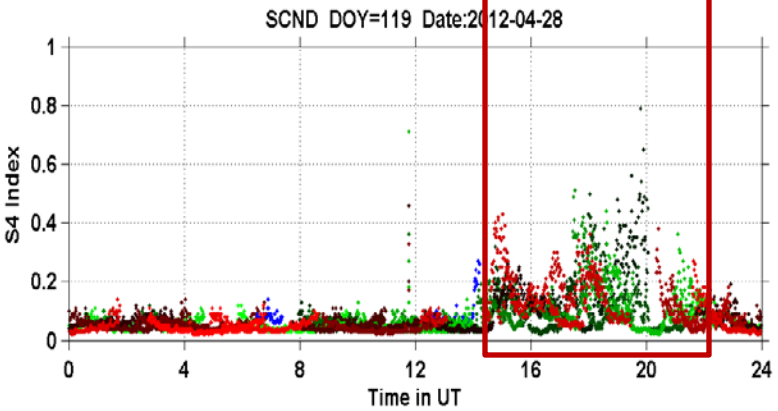

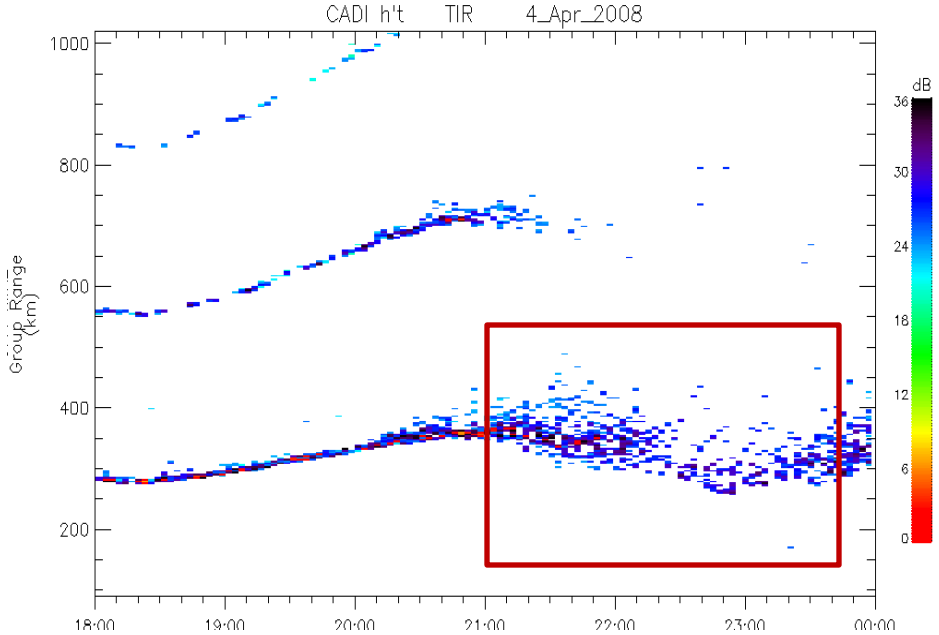

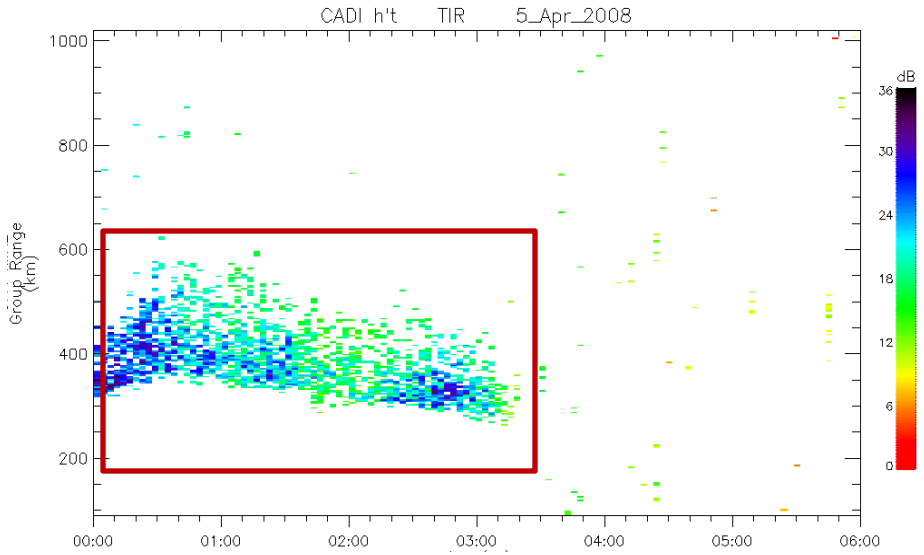

Week L-band scintillations but strong spread F in ionograms

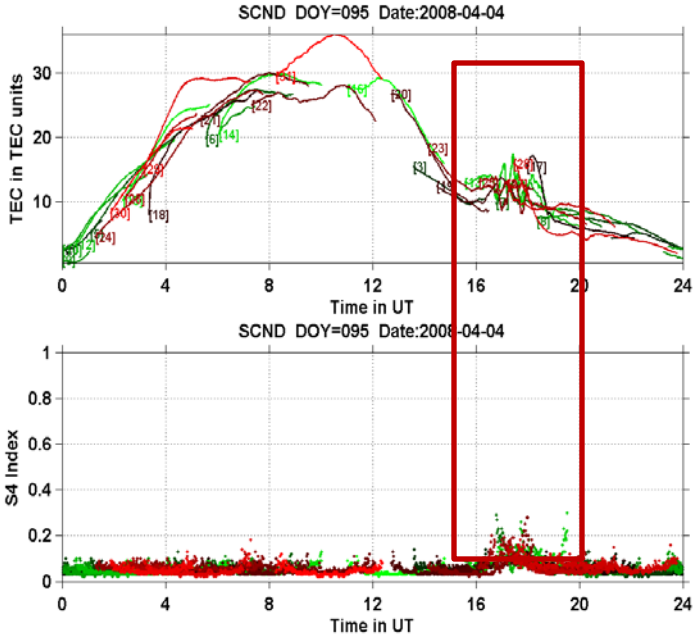

Signature of strong scintillations under evening CEJ event

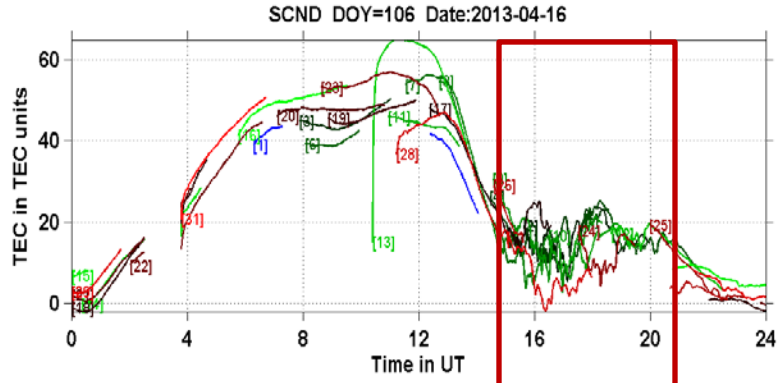

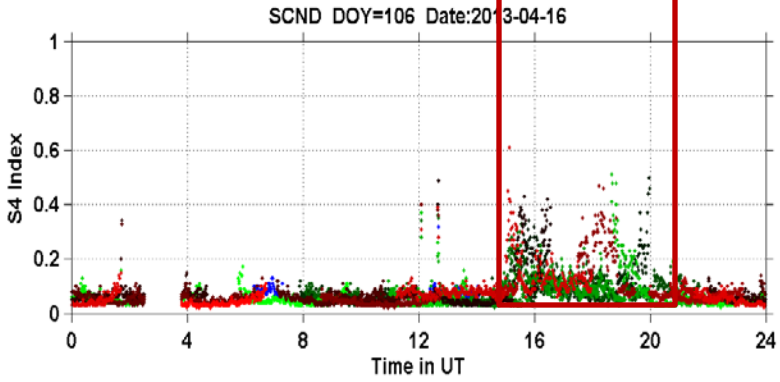

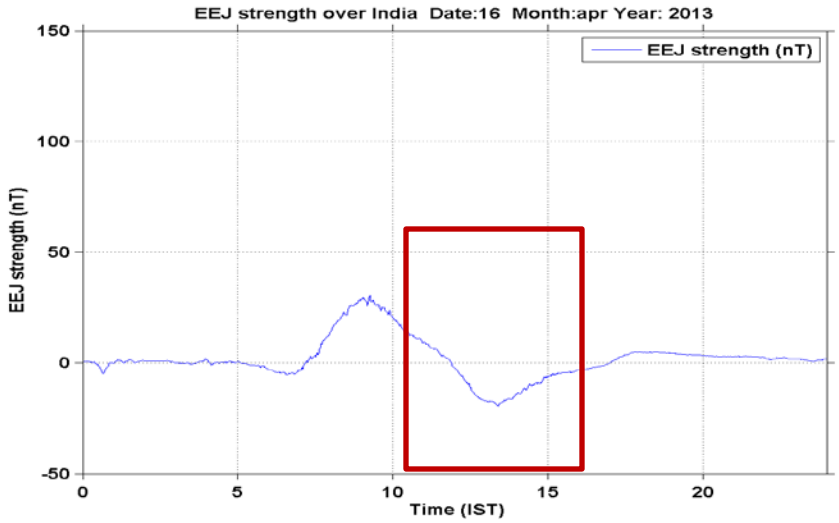

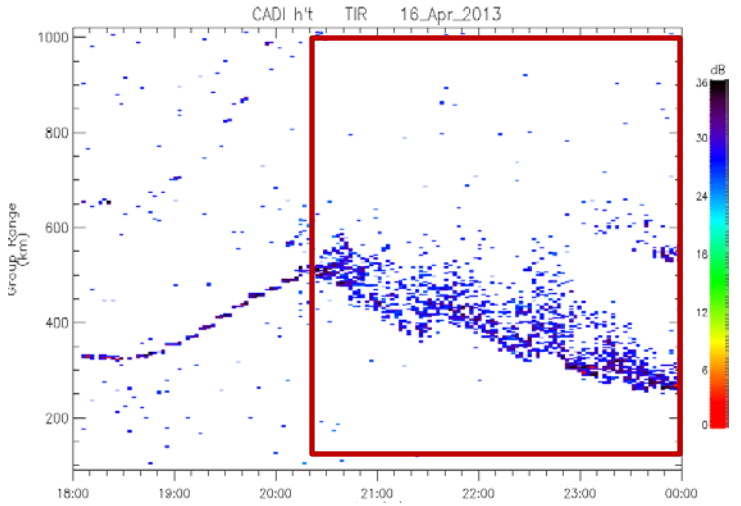

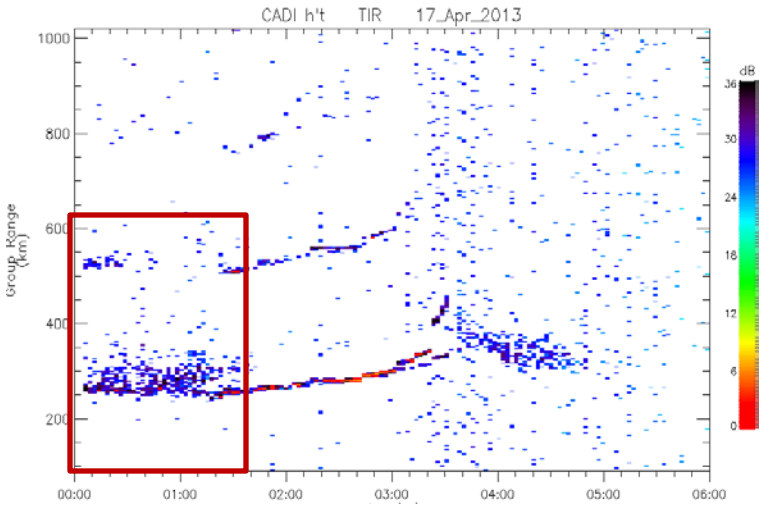

Radar RTI map

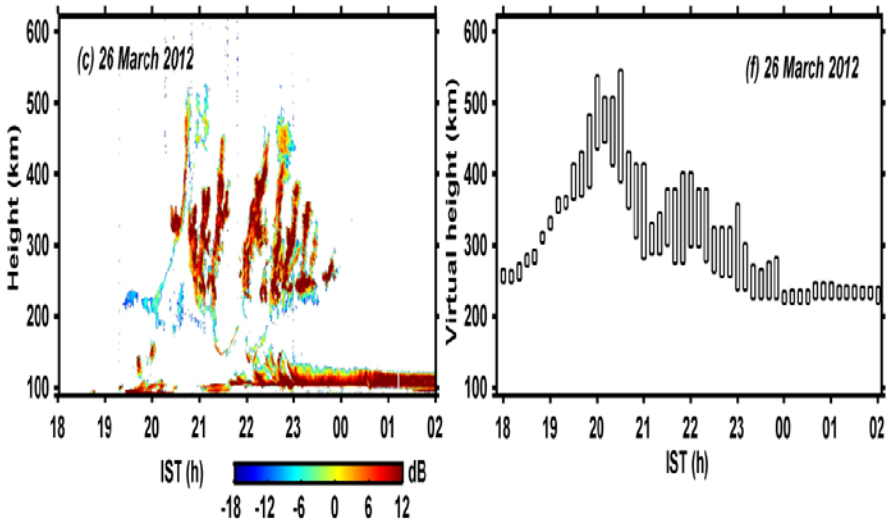

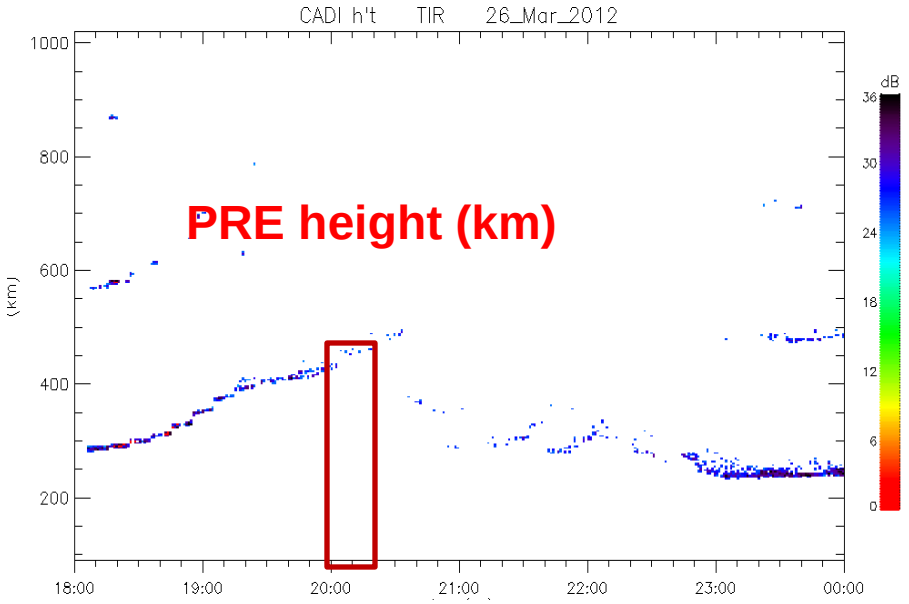

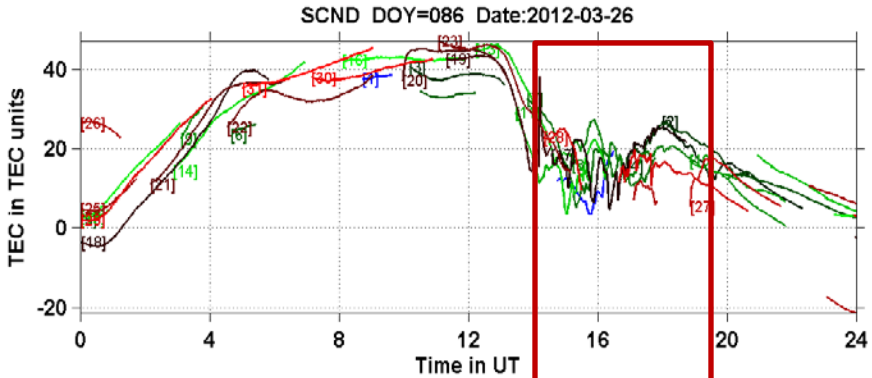

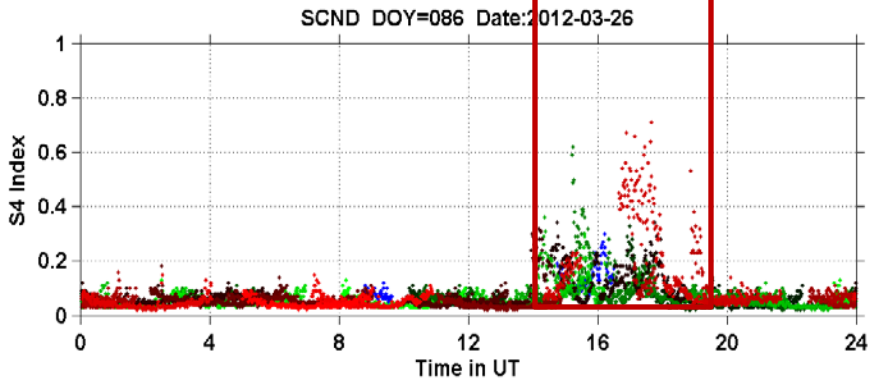

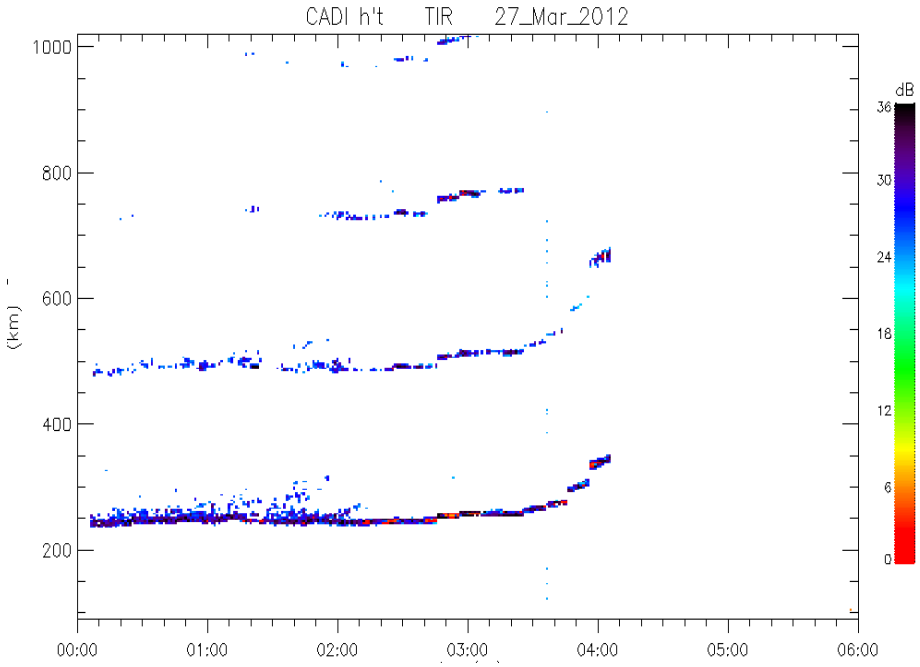

Seasonal and day-to-day variation of Drifts, virtual height, L-band scintillations and spread F during the year 2011

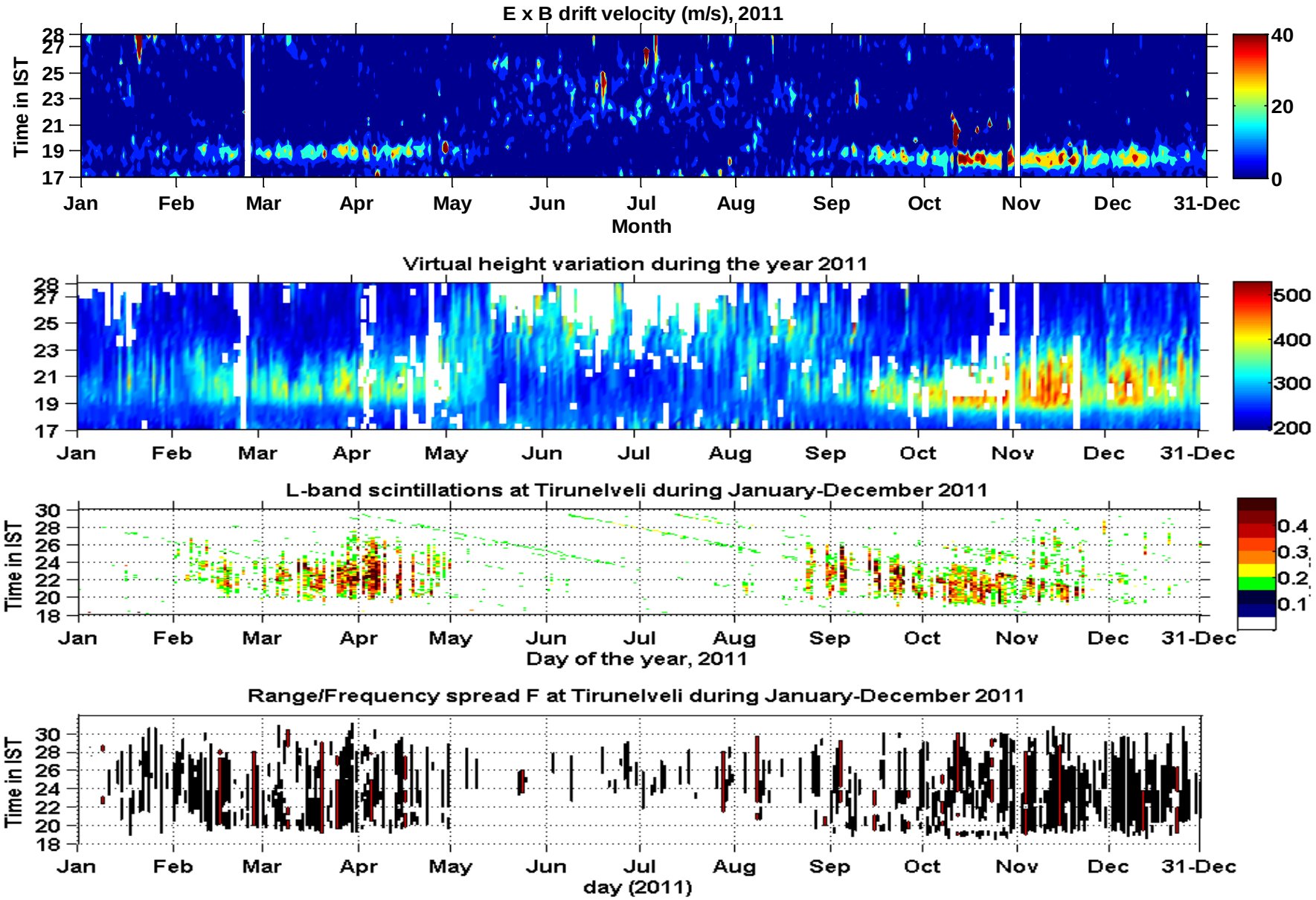

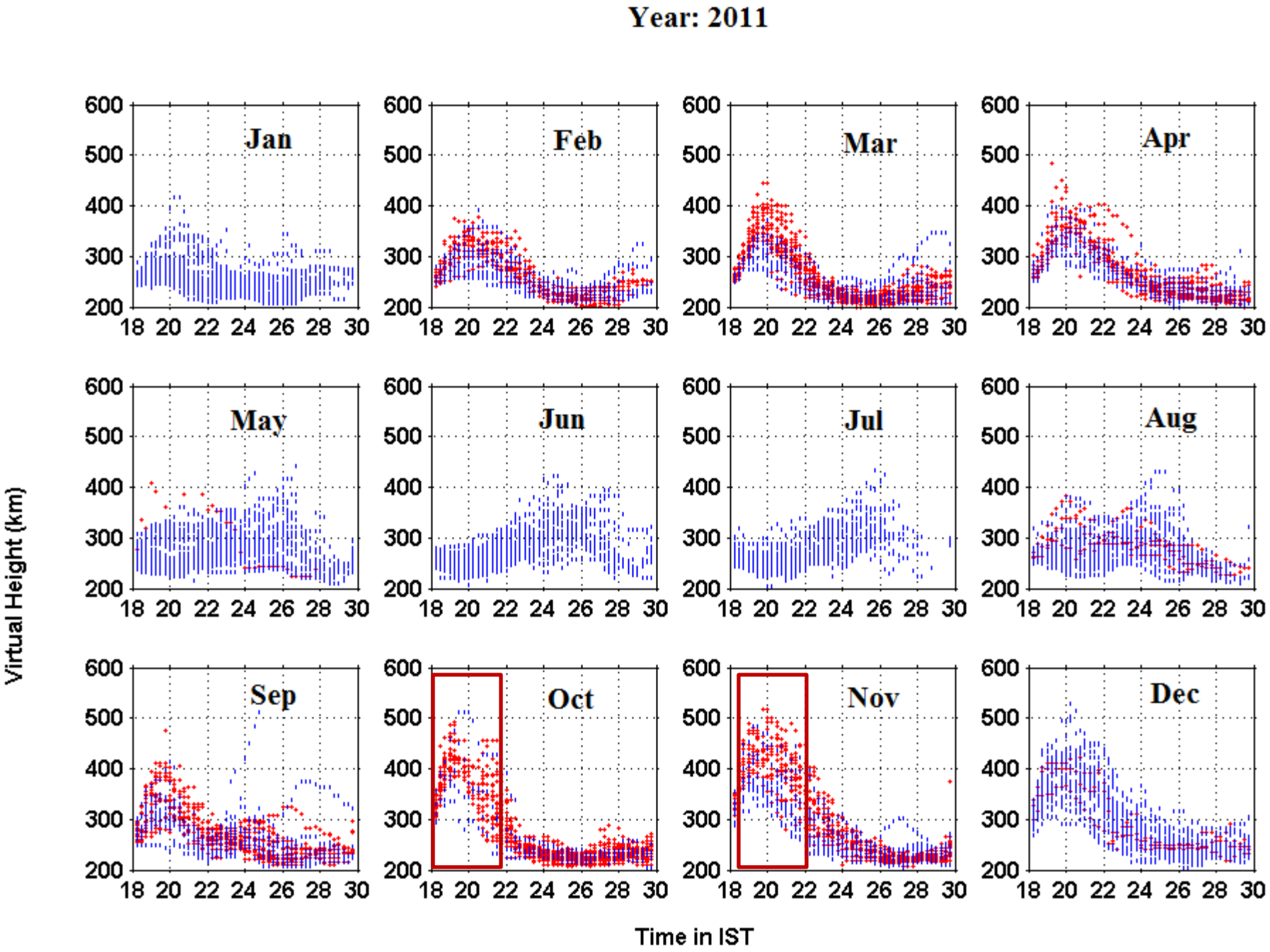
Year: 2011
Jan
Feb
Mar
Apr
May
Jun
Jul
Aug
Sep
Oct
Nov
Dec
600
500
400
300
200
18 20 22 24 26 28 30
Virtual Height (km)
Time in IST

Strength and duration of GPS scintillations (2011)

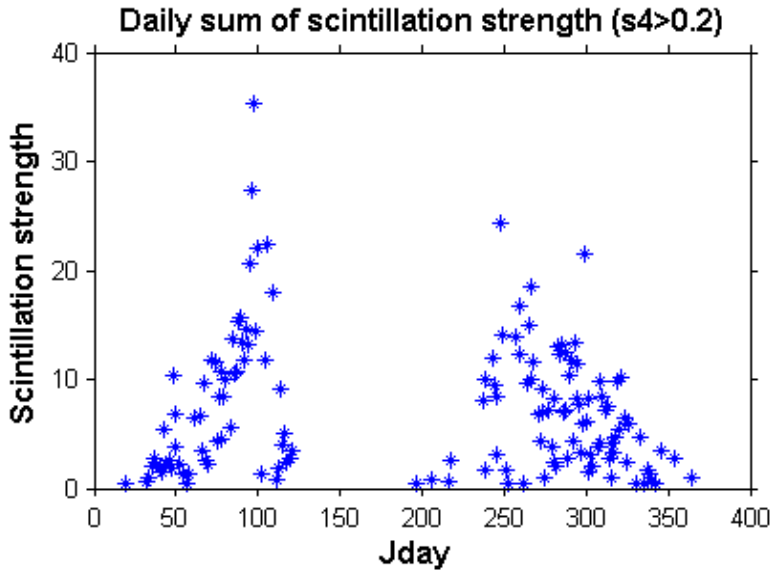

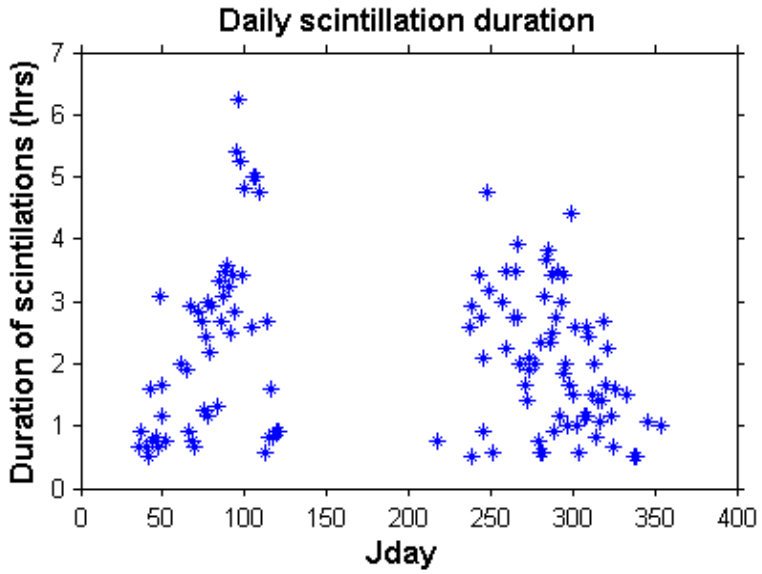

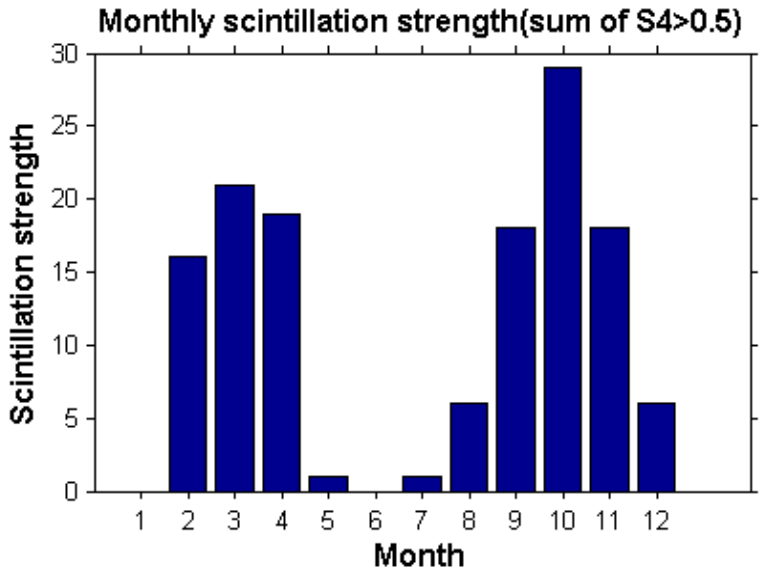

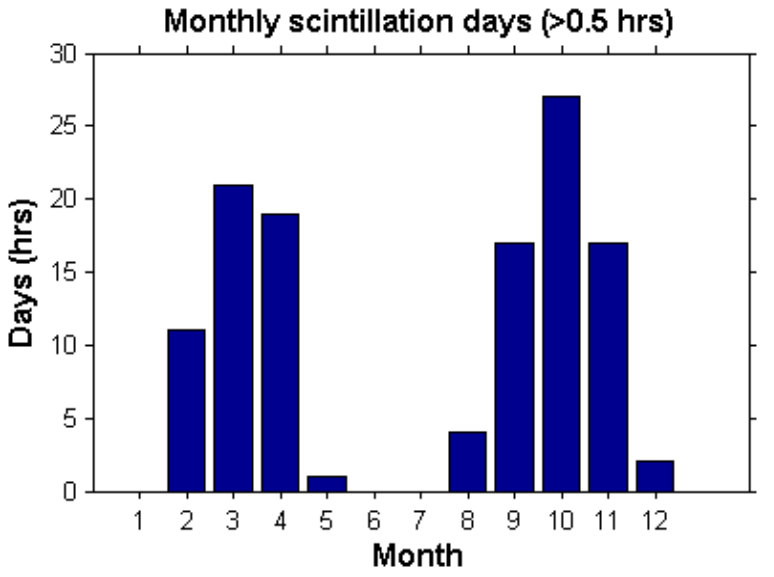

Occurrence of ESF irregularities at different scales (2011)

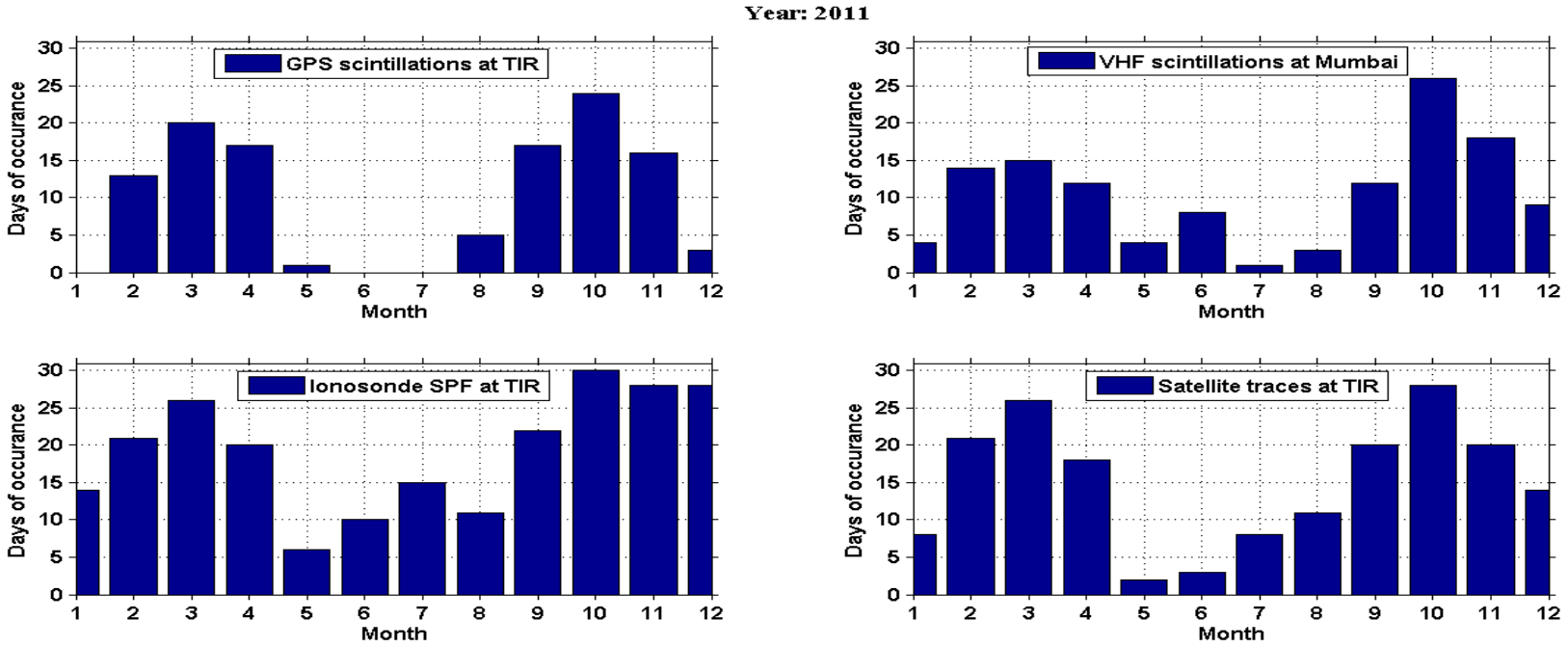

Linear growth rate calculations for the year 2011

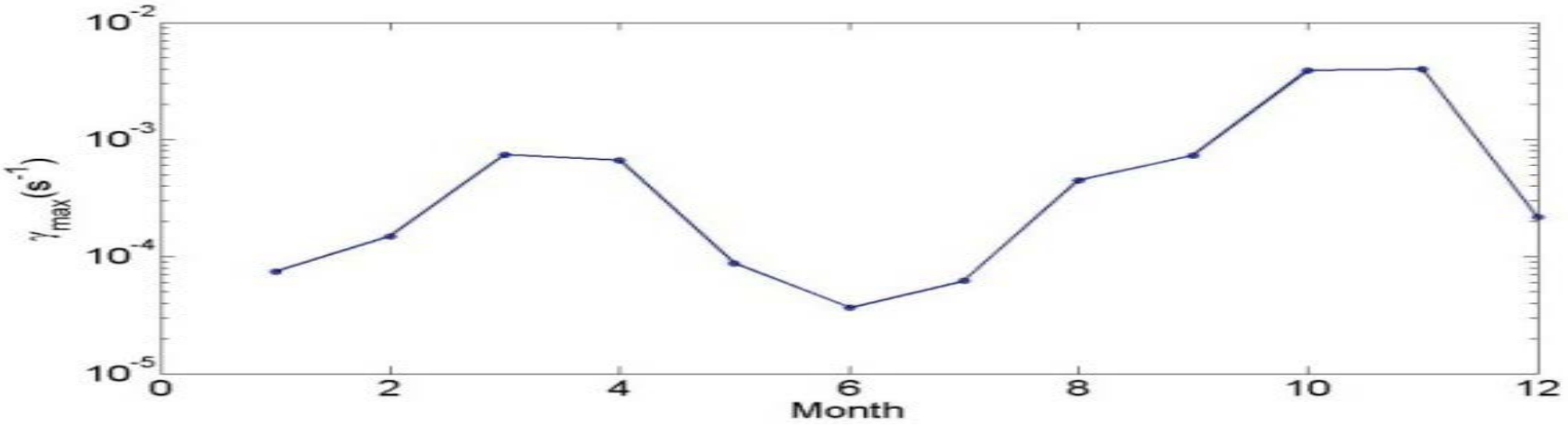

Seasonal and day-to-day variation of Drifts, virtual height, L-band scintillations and spread F during the year 2012

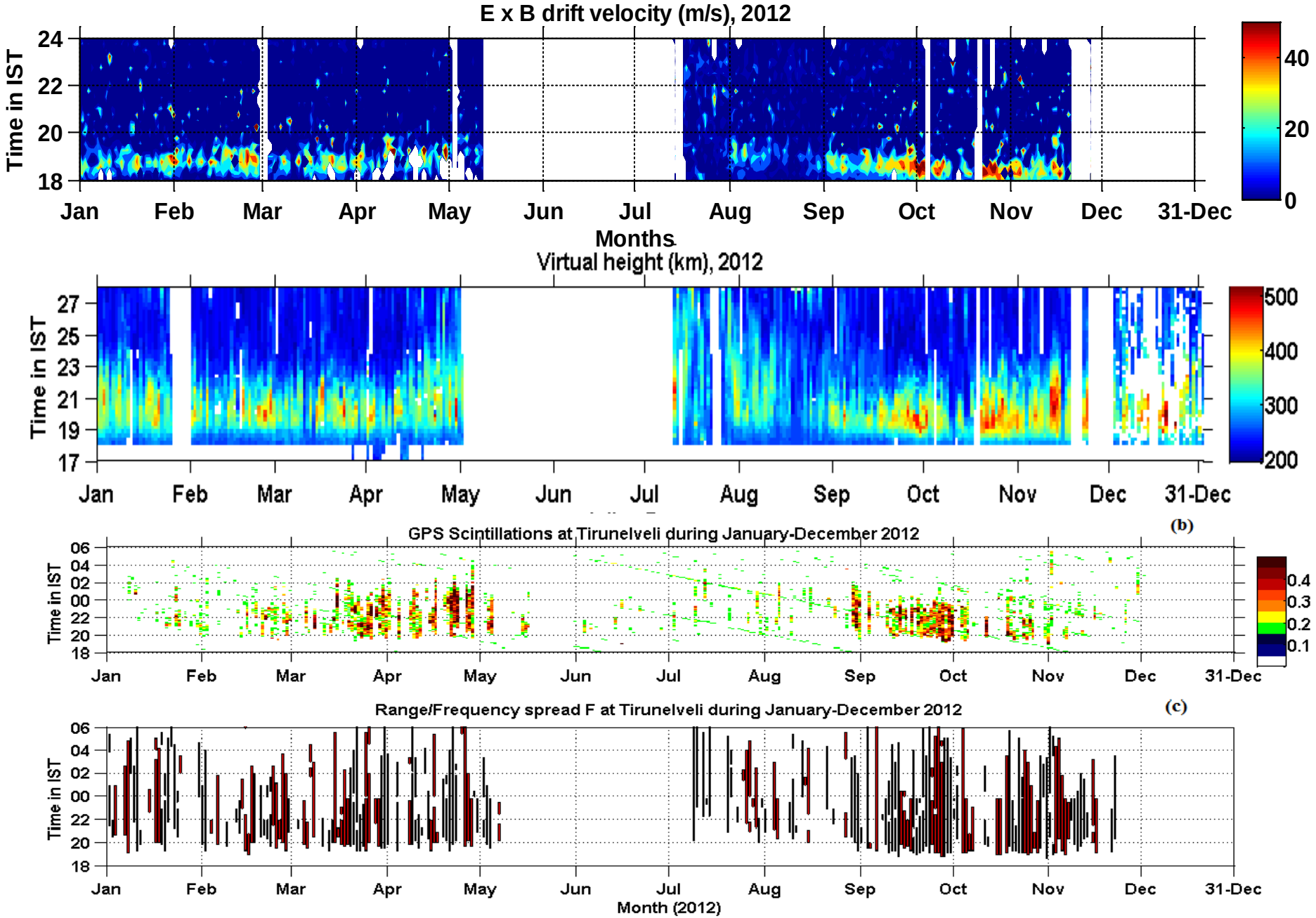

Strength and duration of GPS scintillations (2012)

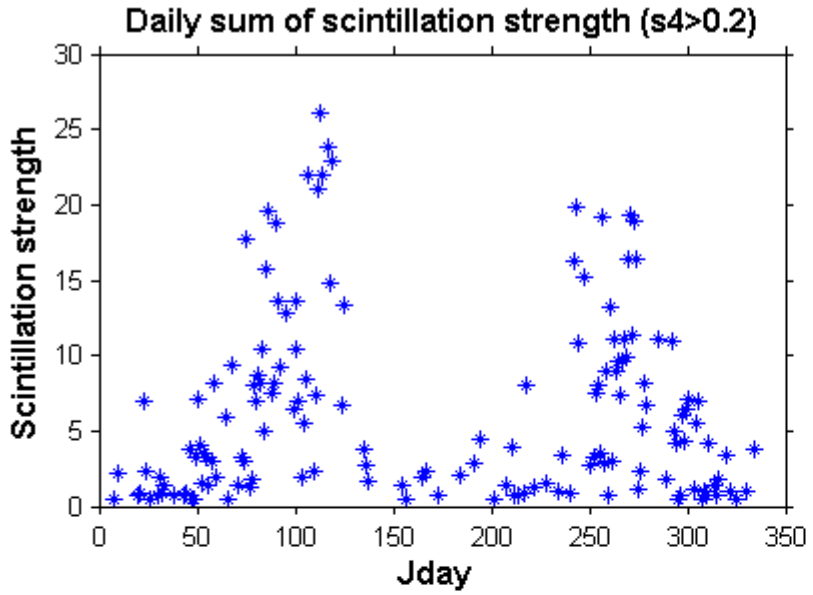

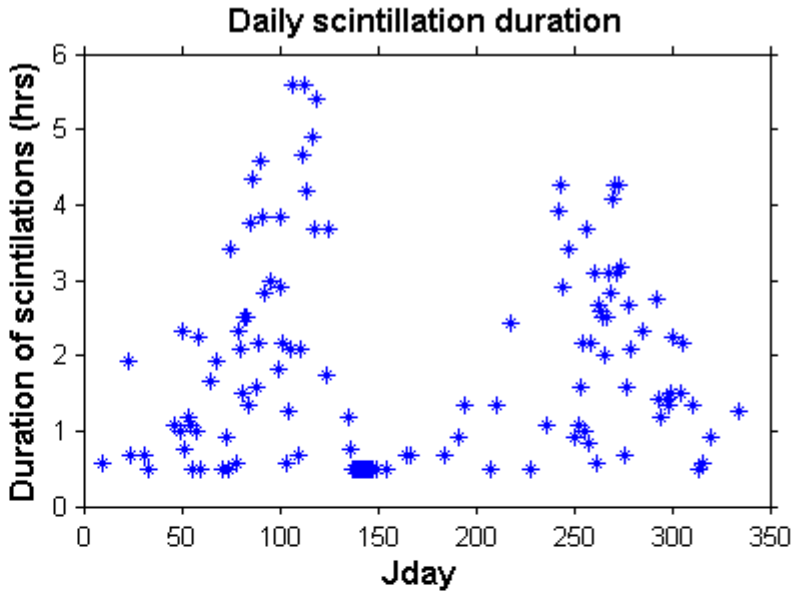

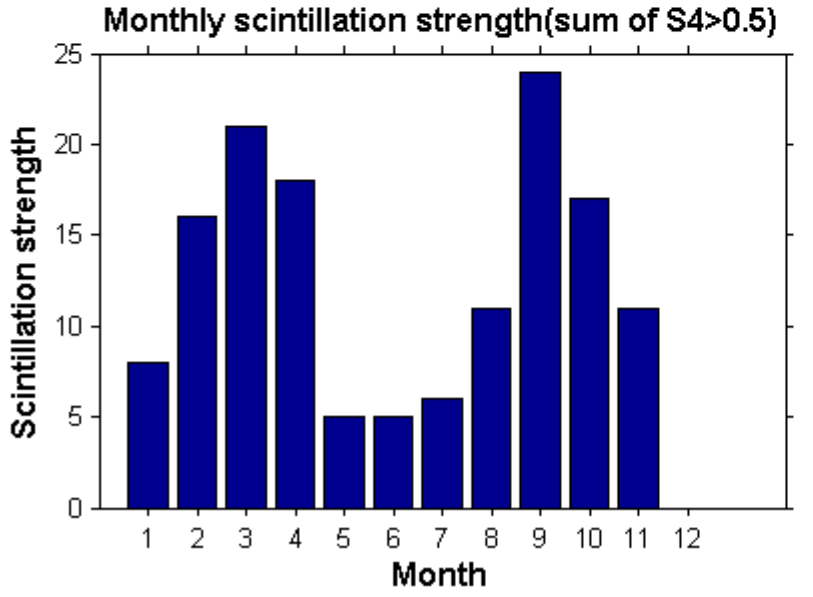

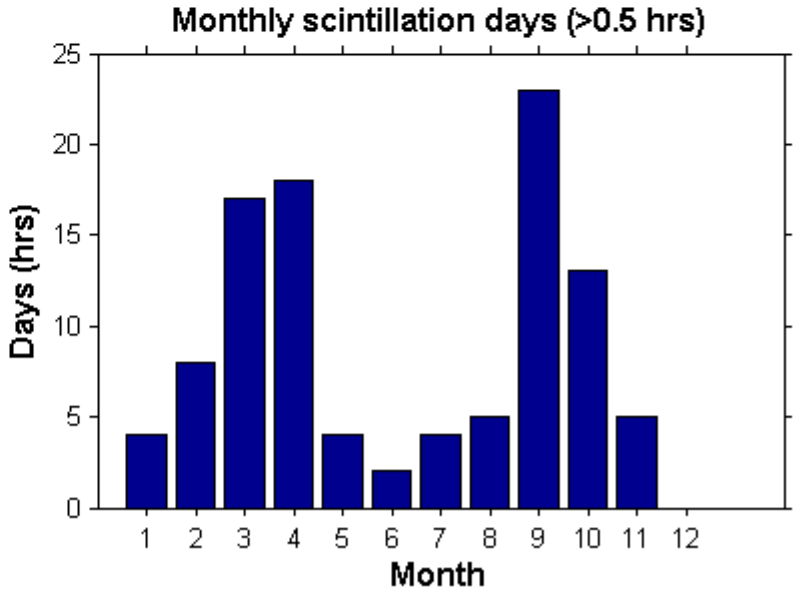

Variation of peak virtual height (indicator of PRE) and time of peak variation during the year 2011

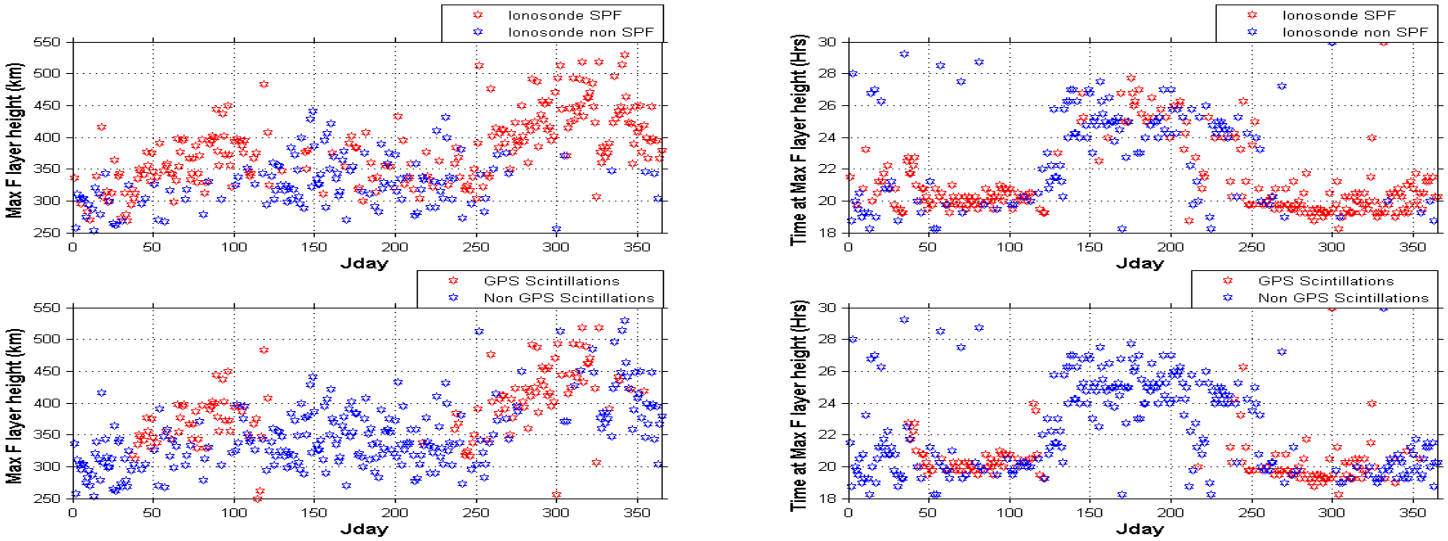

Seasonal and day-to-day variation of max. EEJ during ESF (red) and non ESF days during the year 2011

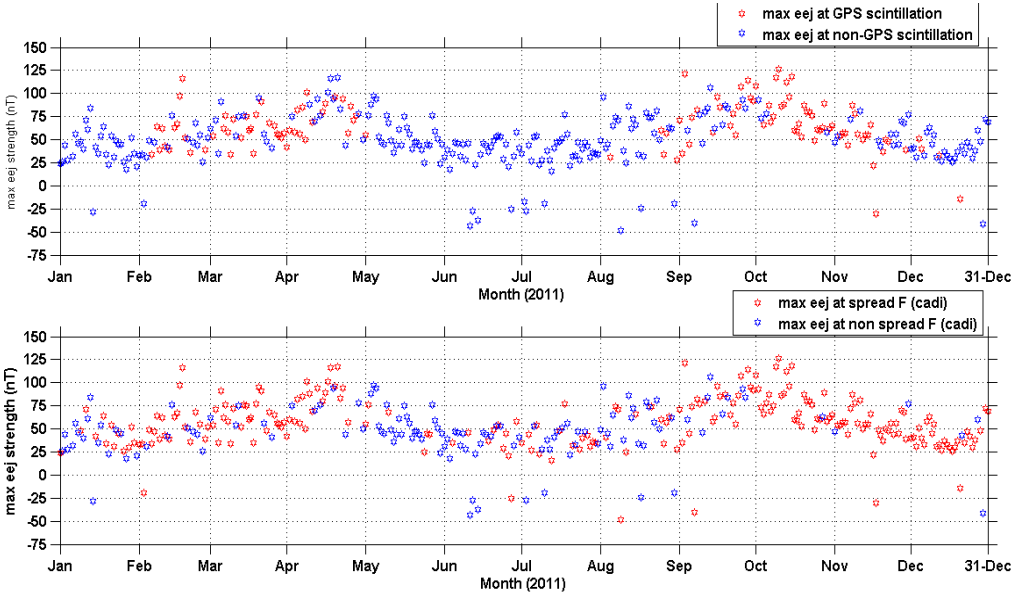

Peak EEJ strength Vs integrated EEJ during scintillations/non scintillations for the years 2011

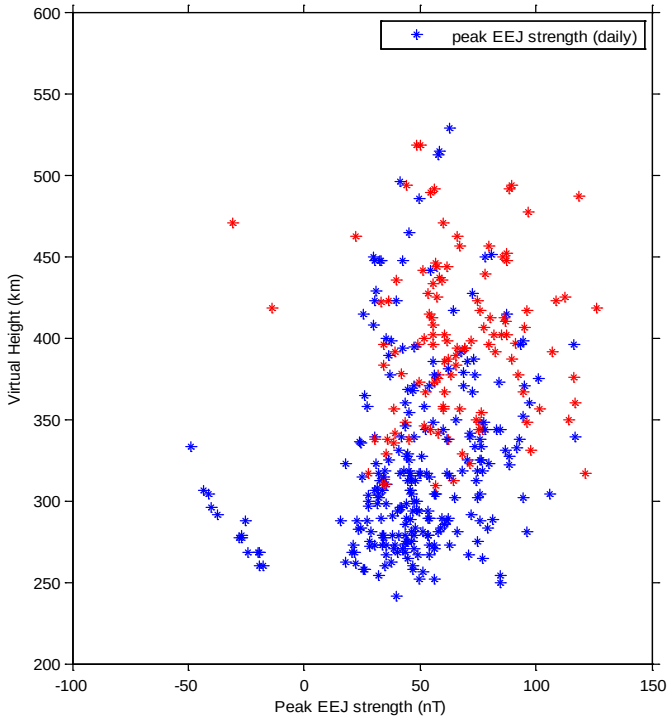

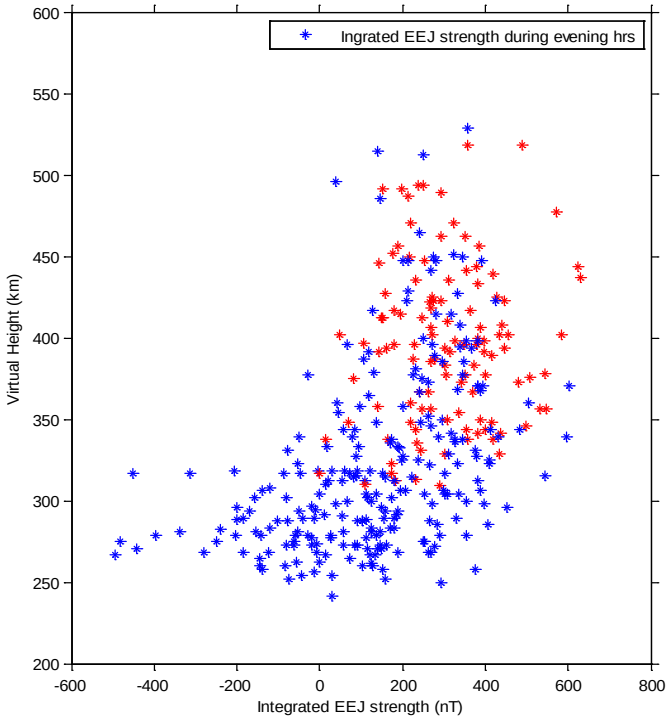

PRE height Vs GPS scintillation occurrence

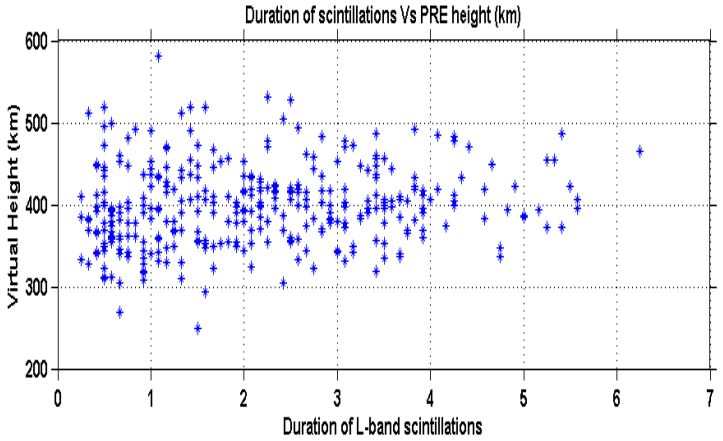

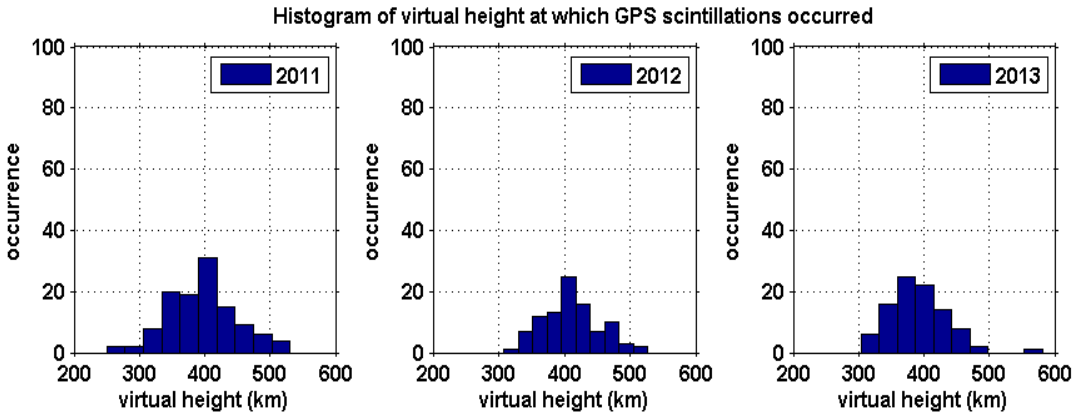

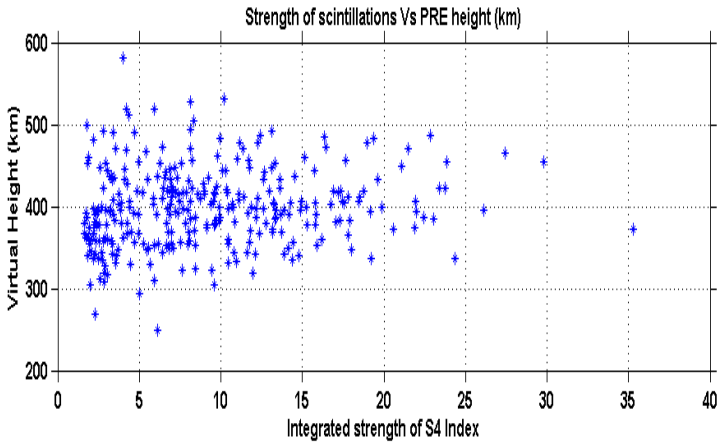

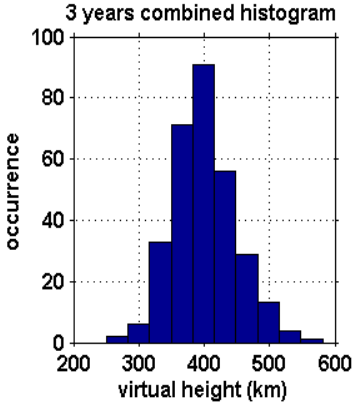

Maximum number of scintillation events are observed when F layer height is located at ~350-400 km altitude.

Summary and conclusions

1. Studied the characteristics of GPS scintillations over Tirunelveli and their relation to ionosonde PRE drifts and to spread F during low to mid solar activity periods.
2. The occurrence of L-band scintillations varied as per the solar flux variations. Scintillations are very weak when solar flux is low. However, as solar flux increased, scintillations start increasing.
3. Our observations also indicate that satellite traces (indication of LSWS) precede the ESF occurrence. Consistent feature of earlier onset of spread F and GPS scintillations during autumn equinox than vernal equinox is noticed. However, longer durations and stronger scintillations are seen in vernal equinox than autumn equinox.
4. The observations indicate that on many occasions post sunset height of the F region is correlated to scintillation activity, while EEJ strength seems to suggest that evening hrs integrated EEJ better correlated with ionospheric scintillations.
5. Our results also suggest that equinoctial asymmetry keep changing.
6. Our results suggest that more scintillation events observed during autumn equinox than vernal equinox which is contrary to previous observations of equinoctial asymmetry. This finding corroborates with enhanced PRE during autumn than vernal equinox.
7. It appears that increase of solar flux during Autumn equinox period may be resulted in the rise in the post sunset height leading to the more spread F occurrences.
8. However, this asymmetry could also be related to symmetry/asymmetry of the crests and related changes in the meridional winds/Integrated Pederson conductivity or asymmetric distribution of vertical drifts in both equinoxes which again depend on solar activity.

Thank you very much for your patience!

Ionosonde Spread F and GPS scintillations during recent St. Patrick's day storm

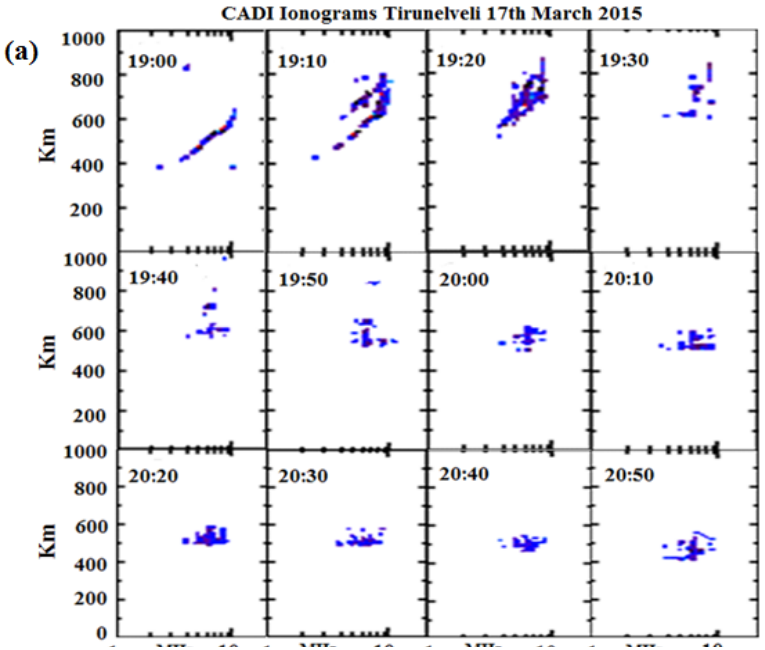

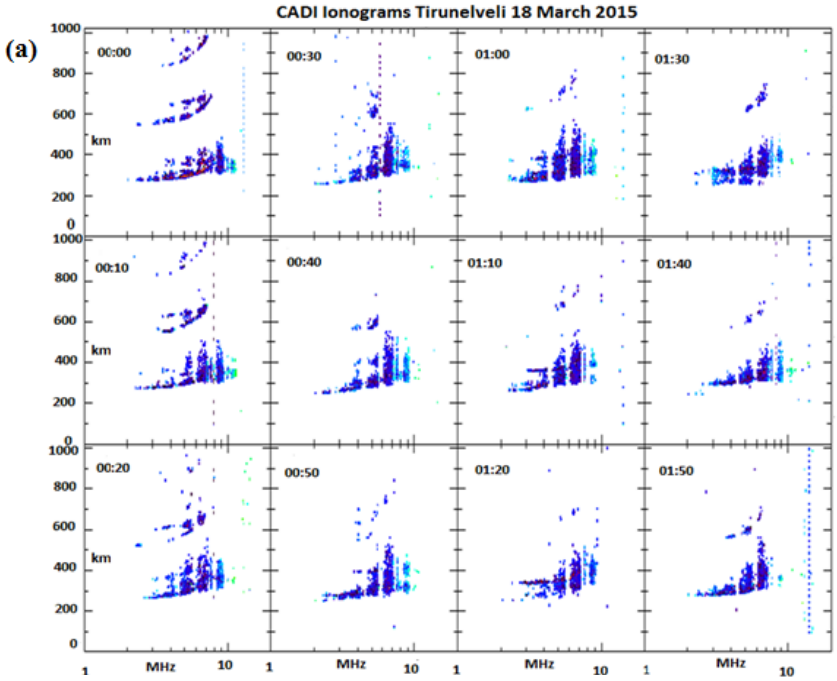

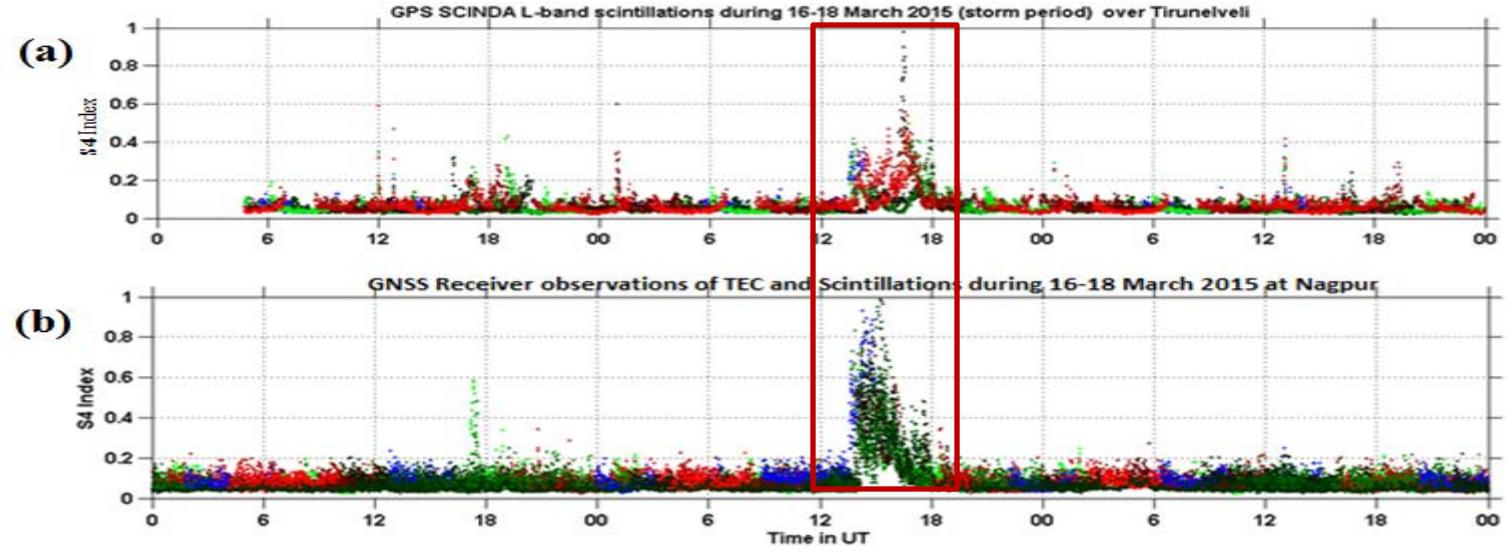

Linear growth parameters used for growth rate calculations

H_{max}

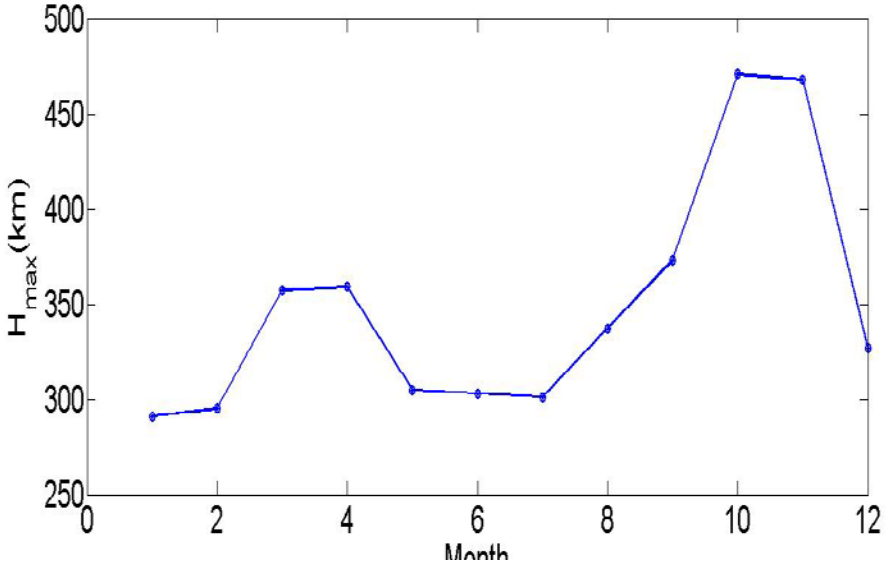

L^{-1}_{max}

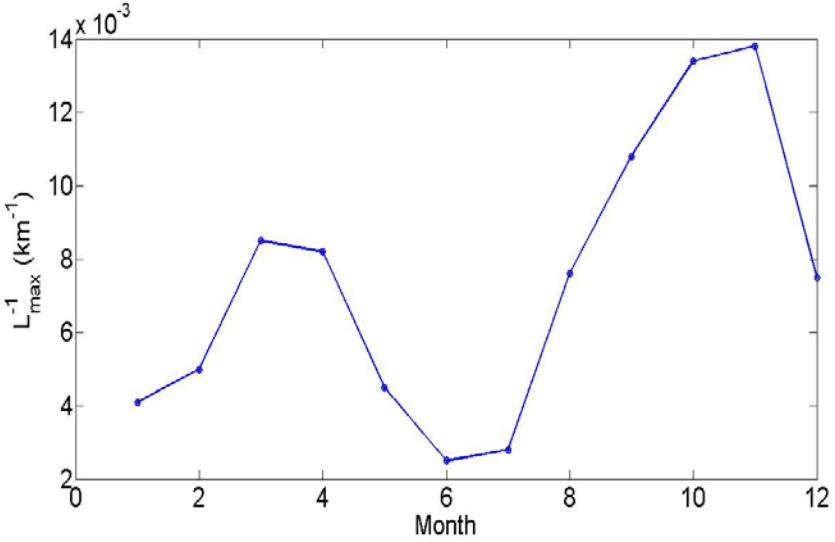

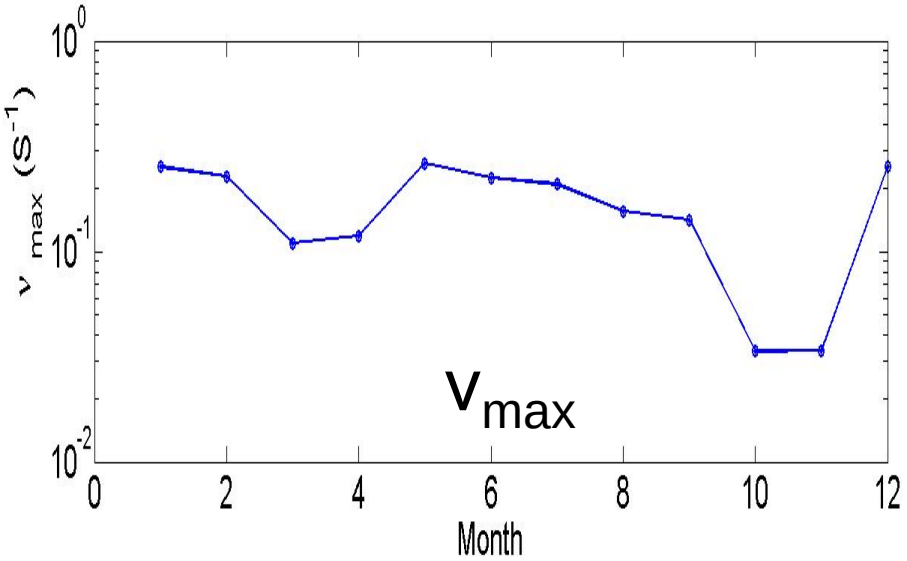

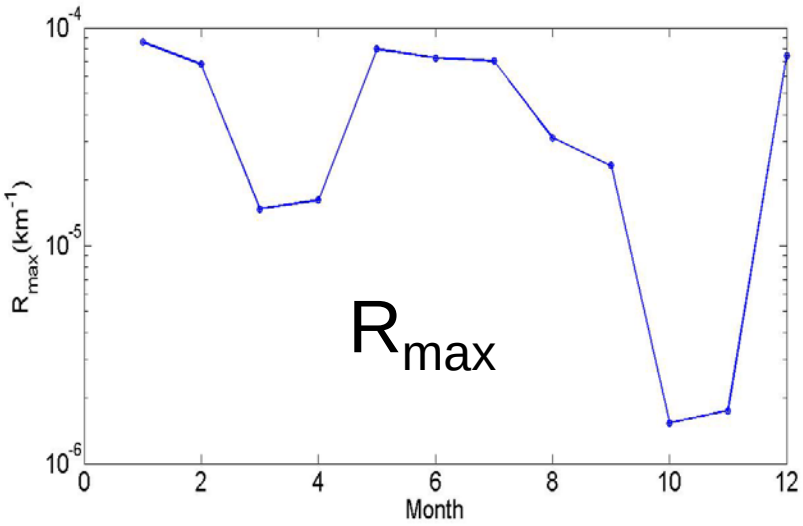

Occurrence of L-band scintillations during the years 2011-2012

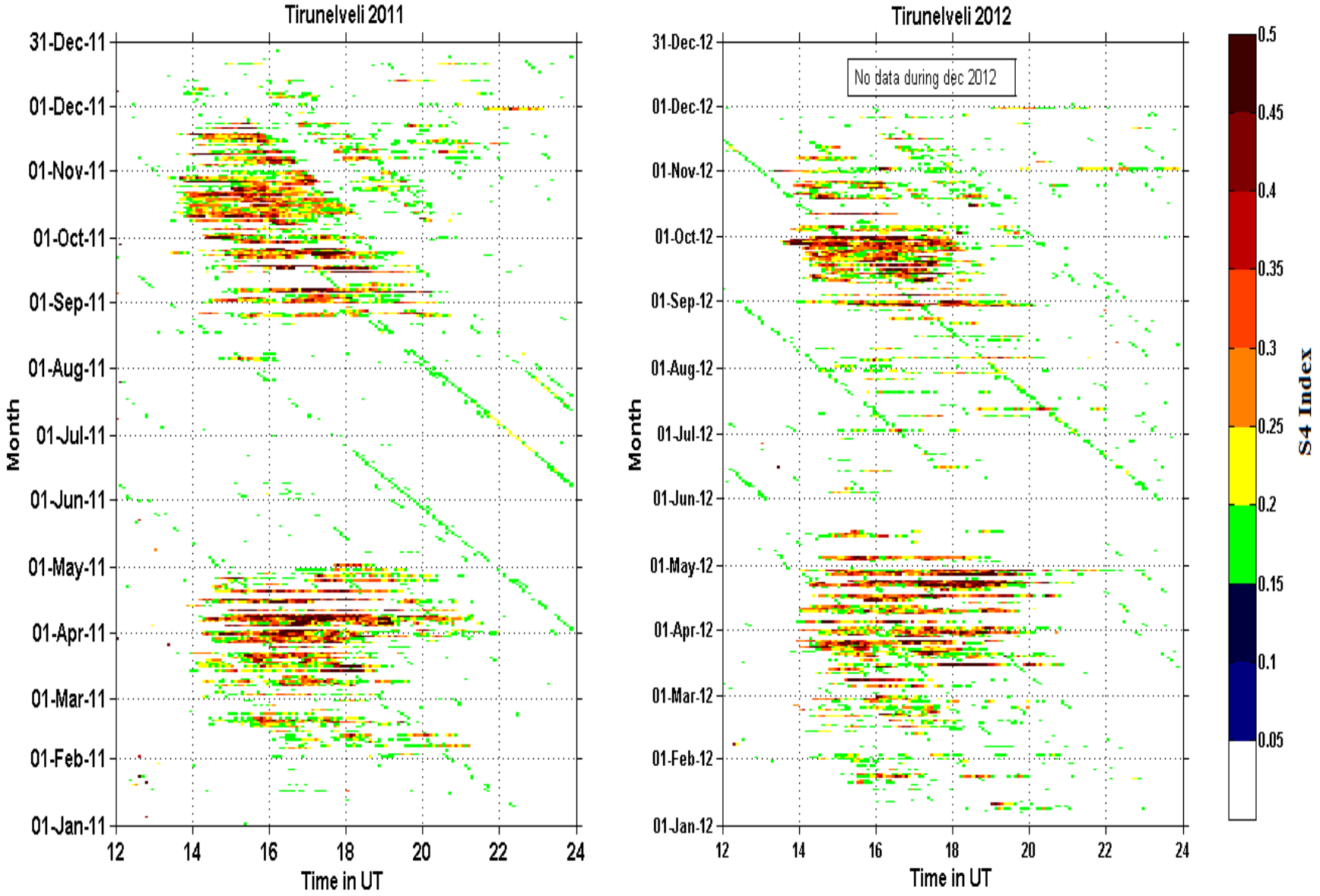

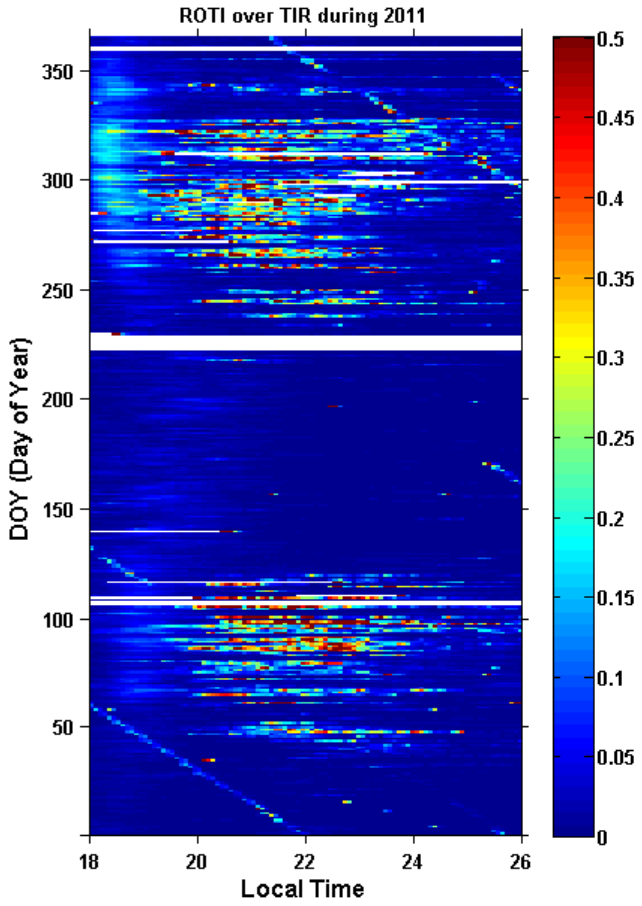
ROTI over TIR during 2011
DOY (Day of Year)
Local Time
350
300
250
200
150
100
50
18
20
22
24
26
0.5
0.45
0.4
0.35
0.3
0.25
0.2
0.15
0.1
0.05
0

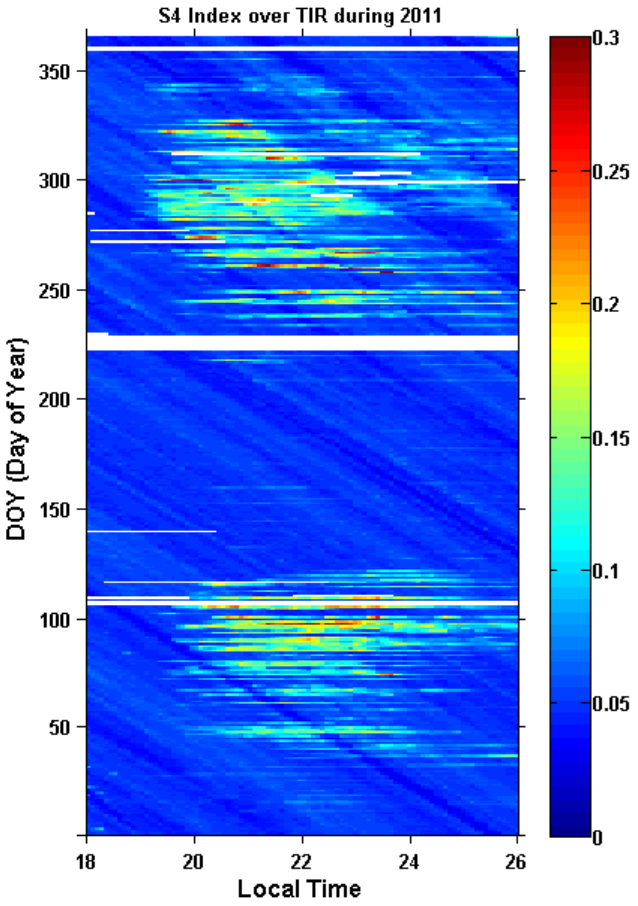
S4 Index over TIR during 2011
DOY (Day of Year)
Local Time
350
300
250
200
150
100
50
18
20
22
24
26
0.3
0.25
0.2
0.15
0.1
0.05
0

The day-to-day, seasonal and latitudinal variation of % occurrence of L-band scintillations during the years (a) 2004 and (b) 2005, respectively. Here the elevation of 30°, longitude of 75°–80° and S4 > 0.2 are used as thresholds.

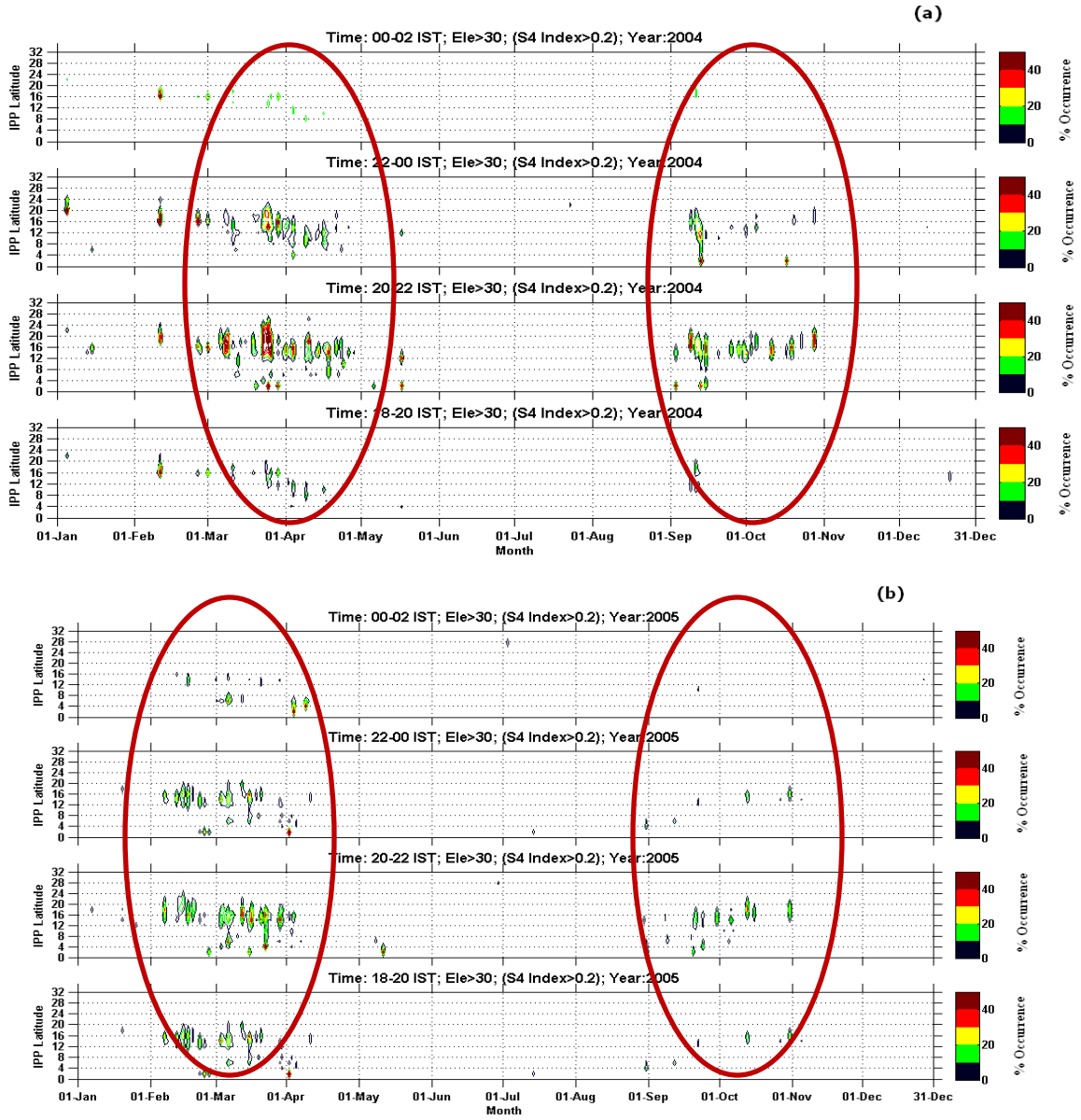

- **Here % occurrence is calculated with a latitude bin of 2 degrees and time interval of every 15 minutes for every day.**

- **The ratio between number of data points exceeds S4>0.2 to total number of data points at a particular latitude will give % occurrence at that particular latitude.**

Sripathi et al., JGR, 2011

Histogram of L-band scintillations during vernal and autumn equinoxes at different latitudes during 2004-2005

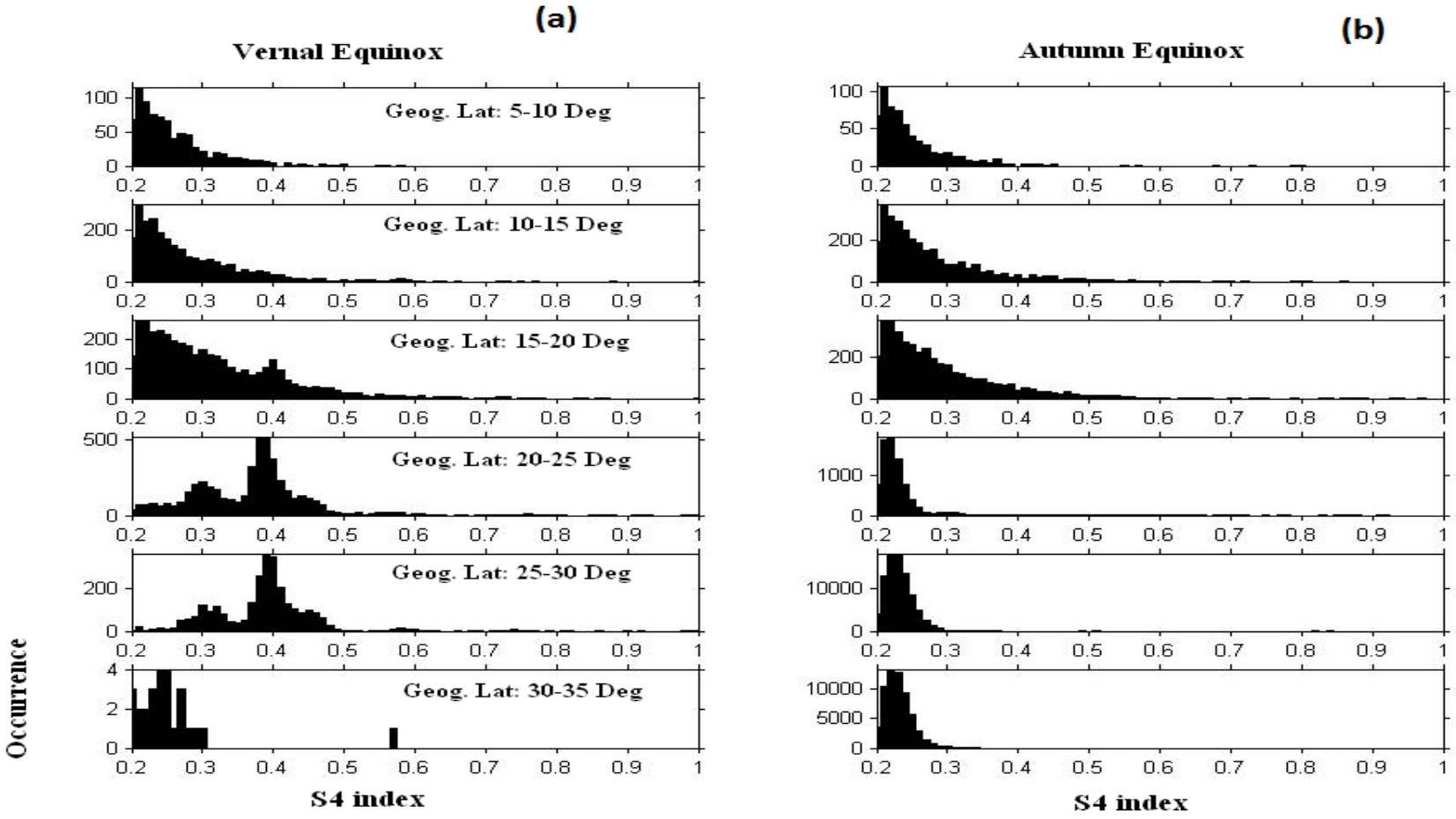

Seasonal and latitude variation of NmF2 over Indian longitude during 2004-2005

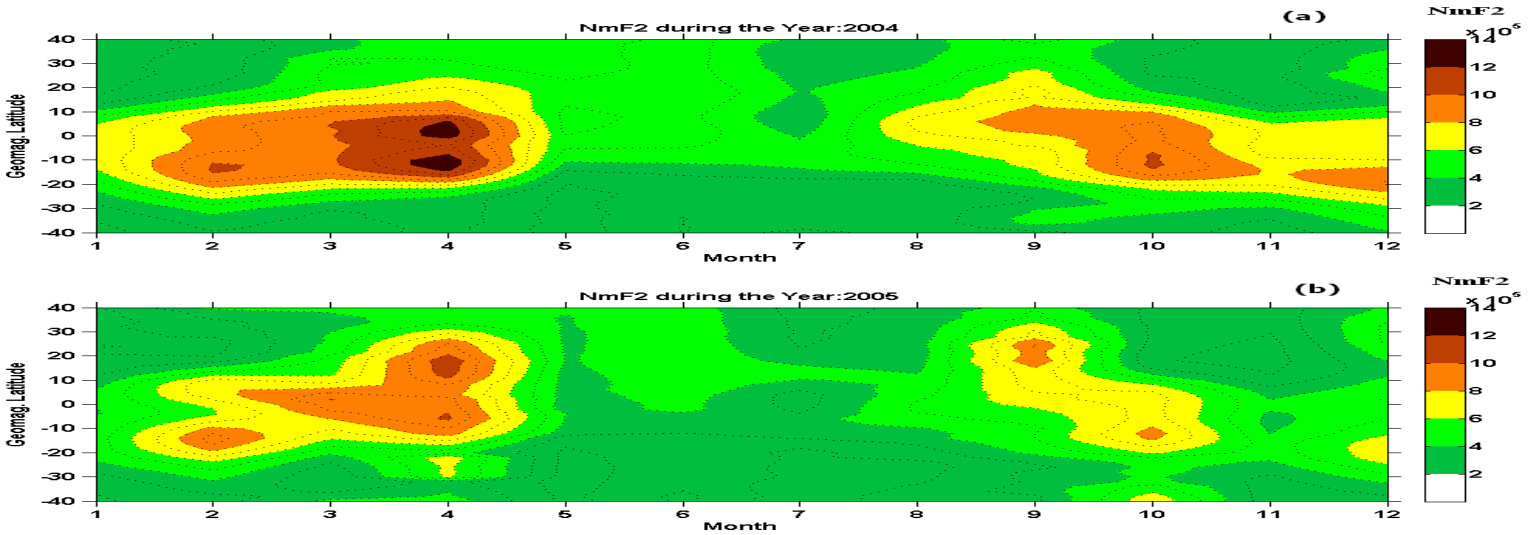

Latitude variation of NmF2 during vernal and autumn equinox during 2004 (Blue) and 2005 (Red)

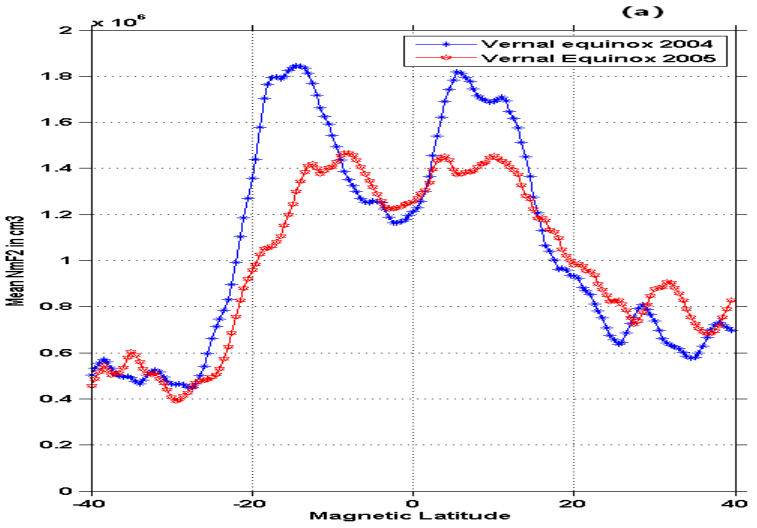

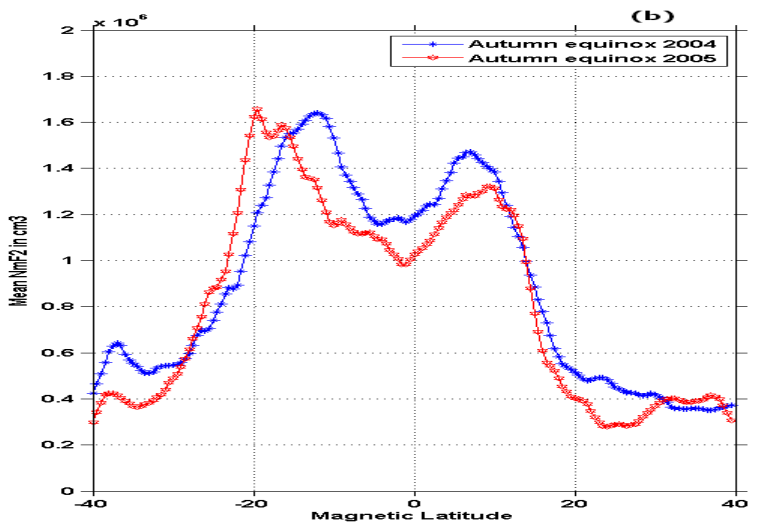

Week scintillations and week spread F in ionogram